

58p

6 1 5

NASA TN D-1594



*on 63-12480  
code-1*

# TECHNICAL NOTE

D-1594

SOME EFFECTS OF SWEEP AND ASPECT RATIO ON THE TRANSONIC  
FLUTTER CHARACTERISTICS OF A SERIES OF THIN CANTILEVER  
WINGS HAVING A TAPER RATIO OF 0.6

By John R. Unangst and George W. Jones, Jr.

Langley Research Center  
Langley Station, Hampton, Va.

NATIONAL AERONAUTICS AND SPACE ADMINISTRATION  
WASHINGTON

February 1963

copy  
1/

to call 1

NATIONAL ADVISORY COMMITTEE FOR AERONAUTICS

TECHNICAL NOTE D-1594

SOME EFFECTS OF SWEEP AND ASPECT RATIO ON THE TRANSONIC  
FLUTTER CHARACTERISTICS OF A SERIES OF THIN CANTILEVER  
WINGS HAVING A TAPER RATIO OF 0.6<sup>1</sup>

By John R. Unangst and George W. Jones, Jr.

SUMMARY

An investigation of the flutter characteristics of a series of thin cantilever wings having taper ratios of 0.6 was conducted in the Langley transonic blowdown tunnel at Mach numbers between 0.76 and 1.42. The angle of sweepback was varied from 0° to 60° on wings of aspect ratio 4, and the aspect ratio was varied from 2.4 to 6.4 on wings with 45° of sweepback.

The results are presented as ratios between the experimental flutter speeds and the reference flutter speeds calculated on the basis of incompressible two-dimensional flow. These ratios, designated the flutter-speed ratios, are given as functions of Mach number for the various wings. The flutter-speed ratios were characterized, in most cases, by values near 1.0 at subsonic speeds with large increases in the speed ratios in the range of supersonic speeds investigated. Increasing the sweep effected increases in the flutter-speed ratios between 0° and 30° followed by progressive reductions of the speed ratios to nearly 1.0 as the sweep was increased from 30° to 60°. Reducing the aspect ratio from 6.4 to 2.4 resulted in progressively larger values of the flutter-speed ratios throughout the Mach number range investigated.

INTRODUCTION

Several flutter investigations have been made in the Langley transonic blowdown tunnel in order to provide experimental data on wing flutter in the transonic speed range. The results of the initial investigation, which show that reliable flutter data can be obtained from the slotted-throat Langley transonic blowdown tunnel, are presented in reference 1.

---

<sup>1</sup>Supersedes declassified NACA Research Memorandum L55I13a by John R. Unangst and George W. Jones, Jr., 1956, and NACA Research Memorandum L53G10a by George W. Jones, Jr., and Hugh C. DuBose, 1953.

In the present investigation, the flutter characteristics of a series of seven systematically varied wing planforms at transonic speeds were studied. The purpose of the investigation was to determine the effects of sweepback and aspect ratio on the flutter speed for Mach numbers in the vicinity of 1.0. The systematic planform variation was accomplished by varying the sweepback from  $0^\circ$  to  $60^\circ$  on wings with an aspect ratio of 4 and varying the aspect ratio from 2.4 to 6.4 on wings with a sweepback of  $45^\circ$ . All the wings had a taper ratio of 0.6 and airfoil sections approximately 4 percent thick. The flutter tests were made at  $0^\circ$  angle of attack over a range of Mach numbers from 0.76 to 1.42. The results are presented and analyzed herein.

#### SYMBOLS

A	aspect ratio including body intercept, $\frac{(\text{Span})^2}{\text{Area}}$
$A_g$	geometric aspect ratio, $\frac{(\text{Exposed span})^2}{\text{Exposed area}}$
a	distance (perpendicular to quarter-chord line) from midchord to elastic axis, expressed as fraction of wing semichord and positive when elastic axis is rearward of midchord
b	semichord perpendicular to quarter-chord line, ft
$b_r$	semichord (perpendicular to quarter-chord line) at intersection of quarter-chord line and wing root, ft
$b_s$	semichord measured streamwise at wing root, ft
EI	bending stiffness, lb-in. <sup>2</sup>
$f_{b,i}$	uncoupled bending frequencies (where $i = 1, 2$ ), cps
$f_{h,i}$	measured coupled bending frequencies (where $i = 1, 2, 3$ ), cps
$f_t$	measured coupled first torsion frequency, cps
$f_\alpha$	uncoupled first natural torsion frequency relative to elastic axis, $f_t \left[ \frac{1 - \left(\frac{x_\alpha}{r_\alpha}\right)^2}{1 - \left(\frac{f_{h,1}}{f_t}\right)^2} \right]^{1/2}$ (except for 245 wing), cps
GJ	torsion stiffness, lb-in. <sup>2</sup>

$g$	structural damping coefficient
$g_h$	structural damping coefficient in bending
$g_\alpha$	structural damping coefficient in torsion
$I_\alpha$	mass moment of inertia of wing section about elastic axis, slug-ft <sup>2</sup> /ft
$k$	reduced frequency, $b\omega/V$
$l$	length of wing panels outside fuselage, measured along quarter-chord line, ft
$M$	Mach number
$m$	mass of wing per unit length along quarter-chord line, slugs/ft
$q$	dynamic pressure, lb/sq in.
$r_\alpha$	nondimensional radius of gyration of wing section (perpendicular to quarter-chord line) about elastic axis, $(I_\alpha/mb^2)^{1/2}$
$V$	stream velocity, ft/sec
$V_e$	measured stream velocity at flutter, ft/sec
$V_e/V_R$	flutter-speed ratio
$V_n$	component of stream velocity perpendicular to quarter-chord line, ft/sec
$V_R$	calculated flutter velocity, ft/sec
$x_\alpha$	distance (perpendicular to quarter-chord line) from wing elastic axis to wing-section center of gravity, expressed as fraction of wing semichord and positive when center of gravity is rearward of elastic axis
$\eta$	nondimensional coordinate along quarter-chord line, measured from intersection of quarter-chord line and fuselage, fraction of length $l$
$\theta$	semichord ratio $b/b_r$ , calculated from $\theta = 1 - \eta(1 - \lambda_p)$
$\Lambda$	angle of sweepback of quarter-chord line, deg
$\lambda$	taper ratio, $\frac{\text{Tip chord}}{\text{Chord in plane of symmetry}}$

$\lambda_p$	taper ratio of panel, $\frac{\text{Tip chord}}{\text{Chord at wing root}}$
$\mu$	mass ratio at $\eta = 0.75$ station, $m/\pi\rho b^2$
$\rho$	air density, slugs/cu ft
$\omega$	angular frequency of vibration, radians/sec
$\omega_{b,i}$	angular uncoupled bending frequency, $2\pi f_{b,i}$ , radians/sec
$\omega_{h,i}$	angular coupled bending frequency, $2\pi f_{h,i}$ , radians/sec
$\omega_\alpha$	angular uncoupled first torsion frequency, $2\pi f_\alpha$ , radians/sec

Subscripts:

Al	aluminum
e	experimental
Mg	magnesium
R	calculated

MODELS

Model Geometry

The models employed represent a series of seven wing planforms varying in sweep and aspect ratio. Five of the planforms had aspect ratios of 4 and sweepback of the quarter-chord line of  $0^\circ$ ,  $30^\circ$ ,  $45^\circ$ ,  $52.5^\circ$ , and  $60^\circ$ . The other two planforms were swept back  $45^\circ$  at the quarter-chord lines and had aspect ratios of 2.4 and 6.4. All wings had taper ratios of 0.6. All wings had NACA 65A004 streamwise airfoil sections except the wing with aspect ratio of 4 and sweepback of  $60^\circ$ , which was approximately 5 percent thick. The ratio of the diameter of the model-mounting sting to the wing span varied from 0.31 for the aspect-ratio-2.4 wings to 0.18 for the aspect-ratio-6.4 wings. Drawings of the various planforms tested are presented in figure 1. Each of the planforms is designated by a three-digit number; the first digit refers to the aspect ratio to the nearest integer and the last two digits refer to the angle of sweepback to the nearest degree. For example, the wing of aspect ratio 4 with  $45^\circ$  of sweepback is designated the 445 wing.

## Materials and Construction

The models were of solid construction rather than built-up rib-and-spar hollow construction. Various materials were used for the models in order that the different planforms might all have flutter speeds within the dynamic-pressure and Mach number capabilities of the wind tunnel. The 400 wings and the 445 wings were made of compreg, a laminated, compressed, resin-impregnated maple. The 430 wings, models 2 and 3 of the 445 wings, and the 452 wings had a compreg core wrapped with a 0.006-inch layer of Fiberglas. Models 1 to 4 of the 460 wings were of compreg wrapped with an 0.018-inch layer of Fiberglas. The remaining 460 wing, model 5, was made of aluminum alloy perforated with a pattern of holes to achieve the desired stiffness distribution. The holes were uniformly distributed over the wing planform and were filled with rubber to obtain a continuous wing surface without appreciably altering the stiffness of the perforated wing (ref. 2 discusses this method of construction in detail). The 245 wing had a tapered core of pine, 2 percent thick, with the grain direction parallel to the quarter-chord line. This core was sandwiched between two layers of balsa, 1 percent thick, with grain direction parallel to the airstream. The 645 wing was made of solid magnesium.

The wings that were wrapped with Fiberglas were made undersize prior to wrapping in order to obtain the desired thickness, but after the 460 wings were covered with Fiberglas their streamwise airfoil sections averaged a maximum thickness of 5 percent instead of the intended 4 percent.

## Physical Parameters

The elastic-axis location, the location of the section center of gravity, the structural damping coefficient in bending, the spanwise distributions of mass and mass moments of inertia, and the frequencies corresponding to the first three, and in some cases four, natural modes of vibration were measured. The elastic-axis locations were obtained by determining, as nearly as possible, the chordwise position at which a concentrated bending load produced no twist in the wing. For the determination of the elastic-axis locations, each wing was clamped along a line perpendicular to the quarter-chord line and passing through the intersection of the wing trailing edge and the root. The mass, center-of-gravity locations, and mass moments of inertia (or radii of gyration) were obtained from strips of each wing cut perpendicular to the quarter-chord line. The structural damping coefficients were determined from the decrement of free-bending vibrations in still air. Natural frequencies were determined from forced-vibration tests of the wings rigidly mounted on a massive steel bench.

Values of the geometric and physical properties of the models are found in table I. For each planform at least one representative set of physical parameters is presented for each type of model construction. In addition, measurements were made of the spanwise variation of the bending and torsional stiffnesses, EI and GJ, for some of the models. The method of measurement is described in reference 2. The results of the stiffness measurements are given in figures 2 to 7. As indicated in the figure keys, some measurements were repeated and the results give an indication of the repeatability of the method.

## APPARATUS AND TESTS

### Wind Tunnel

The Langley transonic blowdown tunnel, which was used for these tests, is equipped with a slotted, octagonal test section which allows the tunnel to operate from subsonic speeds through and above sonic speed to a Mach number of about 1.45. A plan view of the tunnel with a model installed and a cross-sectional view of the test section are shown in figure 8.

A variable and continuous regulation of the airflow is allowed by a set of three plug valves, located between a high-pressure reservoir and the tunnel, which are operated by a single control. A quick-operating mechanism closes the valves in approximately 1/2 second.

The test-section Mach number is controlled by the valve opening, which governs the stagnation pressure, and by the size of the orifice plate installed downstream of the test section. When choked, an orifice permits a specific test-section Mach number to be maintained as the stagnation pressure, and hence the air density, is varied from the value at which the orifice chokes to the maximum design pressure, 75 pounds per square inch. Since the occurrence of flutter depends on air density as well as velocity and Mach number, this technique, along with proper model design, permits flutter to be obtained throughout the Mach number range on the same model. Figure 9 shows the variation of dynamic pressure as a function of test-section Mach number for three orifice plates. A sufficient number of orifice plates were available to choke the tunnel over a Mach number range between 0.85 and 1.4 in Mach number increments of approximately 0.06. The tunnel could be choked at Mach numbers below 0.85 by attaching inserts to the 0.85 orifice. Mach numbers above approximately 1.4 were obtained by bleeding off part of the air in the tank surrounding the slotted test section. It should be noted that the test-section velocity is not uniquely defined by the Mach number because of the variation of tunnel stagnation temperature with initial reservoir conditions and expansion in the reservoir during each run. The tunnel is equipped with a viewing screen, not shown in figure 8, which allows observers to watch the model throughout the tunnel operation.

### Support System

The wings were mounted at  $0^\circ$  angle of attack on a 3-inch-diameter cylindrical sting fuselage. A fixed wing-root condition was obtained by mounting the wing with close-fitting filler blocks and four 3/8-inch bolts. Figure 10 shows a flutter model mounted on the sting fuselage. The fuselage nose extended into the subsonic flow region of the tunnel entrance cone in order to prevent the formation of a bow shock wave and its associated reflection from the tunnel walls onto the model. The support system was considered to form a rigid mount since the mass of the system was very large compared with the mass of a model. The measured fundamental bending frequency of the support system was approximately 15 cycles per second.

It will be noted in figure 10 that there was a slight bulge in the sting fuselage behind the model. The shock wave which formed near this bulge at transonic speeds may, for a limited Mach number range, have crossed the outer portions of the more highly swept wings, notably the 460 wings. The absence of any consistent irregularities in the experimental data, however, suggests that the presence of this shock wave had a negligible effect on the results.

### Instrumentation

Each model was instrumented with strain gages externally mounted on the wing near the root and oriented so as to distinguish between wing bending and torsion deflections. However, the gages could not be oriented so as to eliminate completely cross coupling between the bending and torsion signals. The strain gages were used to provide an indication of the start of flutter and to obtain a record of the frequency of wing bending and torsion oscillations.

During the tests, a multichannel recording oscillograph was used to make simultaneous recordings of the strain-gage signals, tunnel stagnation pressure and temperature, and test-section static pressure. A sample test record is given in figure 11, in which the start of flutter is shown by the change in the wing oscillations from an irregular form to a near sine wave, the amplitude of which rapidly increased. For some of the tests, the strain-gage signals of each wing were fed into a cathode-ray oscilloscope - the bending signals to the vertical axis and the torsion signals to the horizontal axis. A simple closed geometric pattern resulted at flutter, and this aided the model observer in determining the start of flutter.

A high-speed, 16-mm motion-picture camera (approximately 1,000 frames per second) was used to obtain a visual record of wing deflection during some of the flutter tests. These films served as an aid in defining the mode shape and magnitude of flutter.

### Tests

The objective of the wind-tunnel test program was to determine the flutter characteristics of each wing at  $0^\circ$  angle of attack for several transonic Mach numbers. The procedure followed in obtaining model flutter at a particular Mach number was to increase the stagnation pressure gradually until flutter was seen by an observer viewing the model. The stagnation pressure and, consequently, the Mach number, was then held constant for a brief interval at initial flutter conditions, after which the airflow was quickly stopped in an effort to save the model from destruction. Small adjustments in angle of attack were made when necessary in order to trim the models to the zero-lift condition.

## METHODS OF ANALYSIS

### General Considerations

A true indication of the effects of planform variation on the flutter speed in the transonic Mach number range cannot be obtained from a simple comparison of experimental flutter speeds. Because of the operating characteristics of the tunnel, the density, and hence the mass ratio  $\mu$ , varied for the different Mach numbers at which flutter was obtained. Furthermore, the torsional frequency  $\omega_\alpha$  as well as the nondimensional parameters  $x_\alpha$ ,  $a$ ,  $r_\alpha$ , and  $\omega_{h,i}/\omega_\alpha$  varied for the different planforms and, in some cases, for the different models of the same planform. Therefore, in an effort to separate the effects of planform and Mach number variation from the effects of these other variables, the results are presented as  $V_e/V_R$ , the ratio of experimental flutter speed to calculated, or reference, flutter speed, plotted as a function of Mach number (as set forth in ref. 3) for the various planforms.

### Reference Flutter Speed

The method of calculating the reference flutter speeds is based on an analysis of the type presented in reference 3. Briefly, the procedure as applied in this paper employs two-dimensional incompressible aerodynamic coefficients in a Rayleigh-type analysis in which the flutter mode is approximated by the superposition of uncoupled, free vibration modes of a uniform cantilever beam. The aerodynamic coefficients are based on the component of the free-stream velocity normal to the quarter-chord line. The spanwise derivative of the velocity potential, which appears in the method of reference 3, has been neglected.

The effective wing root and tip are defined in the present analysis as the perpendiculars to the quarter-chord line at the intersections of the quarter-chord line with the actual root and tip, respectively.

The values of  $k$  were weighted along the span in accordance with the wing taper, and the spanwise variations of the Theodorsen functions  $F(k)$  and  $G(k)$  were approximated by a straight line between the root and tip values. The solution of the flutter stability determinant was obtained in the form of the structural damping coefficient  $g$  as a function of  $V_n/b_r\omega_\alpha$ . The structural damping coefficient used was that measured in bending with the assumption that  $g_h = g_\alpha = g$ .

Initial  $V_R$  calculations were based on a flutter mode approximated by the uncoupled first bending and first torsion modes of a uniform cantilever beam. These calculations resulted in flutter-speed ratios which were considerably below 1.0 in the subsonic and low supersonic speed range for wings with relatively high values of  $l/2b_r$ . Examination of motion pictures showing the mode shape at flutter, and the proximity of  $\omega_{h,2}$  to  $\omega_\alpha$  for some of the wings, suggested that the inclusion of higher modes in the calculations might result in better agreement

between experimental and calculated flutter speeds at subsonic Mach numbers. Calculations of  $V_R$  were accordingly made by using the uncoupled first and second bending and first torsion uniform cantilever modes for the 445, 452, 460, and 645 planforms. In addition, a four-mode analysis was made for a few of the points for the 460 wing, the fourth mode being the third uncoupled bending mode. Only the first bending and torsion modes were used in the calculations for the other wings.

The measured frequencies of the predominantly bending modes were taken to be the uncoupled values, except for the 245 wing, whereas the measured frequencies of the predominantly torsion modes were adjusted to the uncoupled values. For all the wings except the 245, the uncoupled torsion frequency was inferred from the coupled values by the simplified formula given in reference 3 and in the "Symbols" section herein. Since the vibration modes of the 245 wing were highly coupled, the uncoupled torsion and bending frequencies were determined from the measured coupled values for this wing by means of a Rayleigh-type analysis in which the first three coupled wing modes were expressed in terms of the uncoupled first and second bending and first torsion modes of a uniform cantilever beam. A number of calculations indicated that, in comparison with the more elaborate method employed for the 245 wing, the simplified uncoupling formula of reference 3 was entirely adequate for the other wings.

## RESULTS

### General Comments

Visual observations, examination of high-speed motion-picture films and oscillograph records, and comparison of flutter frequencies with natural frequencies indicated that the flutter obtained in the tests was of the classical bending-torsion type. The wing oscillations at flutter, however, did not necessarily show a continual increase in amplitude with increasing time, but rather reached a constant amplitude. It was also noted that the flutter characteristics of the wings at subsonic speeds differed from those at supersonic speeds. Flutter at high subsonic Mach numbers, near 0.85, occurred with a relatively large amplitude and low frequency, whereas at supersonic Mach numbers, near 1.3, the flutter occurred with a lower amplitude and a higher frequency.

The beginning of flutter was not always as easily defined as that shown in figure 11, particularly at supersonic speeds. In many cases, the oscillograph records revealed a period of intermittent sinusoidal oscillations in both bending and torsion followed by a period of steady continuous flutter as the tunnel conditions approached and crossed the flutter boundary. A sample oscillograph record of one of the test runs showing this kind of behavior is given in figure 12. For this particular test run, the beginning of a period of intermittent sinusoidal oscillations in bending and torsion might be chosen near point C for both wing panels. At point D the oscillations of the right wing become nearly sustained and the frequencies in bending and torsion appear identical, so that point D is defined as a flutter point. The oscillations of the left wing, however, remain intermittent in character until point E is reached. For cases such as that

illustrated in figure 12, a clear-cut distinction between the period of intermittent oscillations and the start of flutter was difficult to make.

For those cases in which flutter did not exhibit a clearly defined start, time-history studies of the frequencies present in the bending and torsion oscillations were made to assist in defining the flutter point. These studies consisted of envelopes of the frequency spectra in bending and torsion plotted against tunnel dynamic pressure. As an example, a frequency study was made for the test record shown in figure 12 and is presented in figure 13. The frequency values at each labeled point in figure 12 were determined by counting the oscillations over a short period of time (about 0.01 second) at several values of time before and after the chosen point and are indicated in figure 13 by corresponding letters. Any one frequency which seemed to predominate among the various values obtained is shown as the predominant frequency in figure 13, and the highest and lowest frequencies obtained are shown as the boundaries of the frequency envelope. Since the oscillations were counted over a short time interval, there is some degree of judgment involved and the frequency values shown should be considered as only approximate. The points where the predominant bending and torsion frequencies first become equal, as shown by points E and D on figures 13(a) and (b), respectively, are defined as flutter points. The points of initial overlapping of the boundaries of the frequency spectra in bending and torsion (point C in figs. 12 and 13) are arbitrarily defined as the beginning of periods of intermittent sinusoidal oscillations which in this paper are called low-damping regions. These periods should be interpreted as regions of uncertainty in which the wing may or may not have been fluttering. Some indication of the beginnings of the low-damping regions in relation to the points of flutter is given in the later figures of this paper. It should be noted that the amplitude of the intermittent oscillations experienced by the models prior to flutter is dependent upon the aerodynamic and structural damping of the models and upon the magnitude and frequency of the exciting disturbances experienced by the models. Since tunnel turbulence no doubt provides most of the excitation experienced by the models, the magnitude of the intermittent oscillations observed on the models prior to flutter is probably not representative of what would be obtained in free air.

In many cases, the two panels of the same model did not flutter simultaneously. This was quite probably due to differences in physical properties, notably the natural frequencies, between wing panels. In those cases, separate flutter points are presented for the start of flutter for each panel. It was also noted that more than one flutter point frequently occurred during a single run. The reason for this behavior is illustrated in figure 9, which shows that for a given tunnel-orifice condition (in this case, the  $M = 1.25$  orifice was installed), the tunnel-operating curve can intersect the flutter boundary curve of a wing at more than one point. For the example of figure 9, three flutter points would be obtained during the run (points A, B, and C). In such cases, each of the points is presented in the data.

#### Presentation of Results

The results of the investigation are presented in table II and are plotted in figure 14. Table II contains the results of theoretical calculations and experiments with some indication of the different models employed, the behavior

of each wing panel during a particular test run, and values of the pertinent flutter parameters. Column 1 gives the identification numbers of the models employed in obtaining the data. Columns 2 and 3, respectively, show the run number and the chronology of the data points during a particular run. (A single run is defined as one operation of the tunnel, starting with the opening of the valves and ending with the closing of the valves.) Columns 4 and 5 contain a code system describing the behavior of each wing panel at each data point. The following designations are used to describe the data points:

- F flutter
- N no flutter
- D low damping
- E end of flutter with dynamic pressure increasing
- G strain gages inoperative
- X wing panel destroyed or not installed

Subscripts 1 or 2 attached to these designations refer to the first or second occurrence of flutter on the panel during a particular run. For example, a series of data points obtained during a given run might be coded as follows:

Run	Point	Left	Right
3	1	F <sub>1</sub>	F <sub>1</sub>
	2	E <sub>1</sub>	E <sub>1</sub>
	3	D <sub>2</sub>	D <sub>2</sub>
	4	F <sub>2</sub>	D <sub>2</sub>
	5	F <sub>2</sub>	F <sub>2</sub>

In this example: at point 1, both panels started to flutter for the first time; at point 2, both panels stopped fluttering; at point 3, both panels exhibited behavior which has been previously defined as low damping; at point 4, the left panel fluttered a second time during the run but the right panel continued low-damping behavior; and at point 5, the right panel fluttered a second time while the left panel continued to flutter.

Presented in figure 14 are the results of the investigation in the form of plots of the ratio of experimental to calculated flutter speed  $V_e/V_R$  as a function of Mach number for the various planforms tested. The low-damping regions are indicated in these plots by dashed lines extending from the beginning of the low-damping period to the point of definite flutter. The direction of these dashed lines is indicative of the manner in which the speed and Mach number varied as the flutter condition was approached during the tunnel tests. Flutter

is shown in the plots by means of plain symbols, and the ends of flutter periods are indicated by means of shaded symbols.

The following paragraphs contain some general comments concerning the data presented in figure 14 for each of the planforms and, in a few cases, some observations regarding the behavior of the wings during the tests.

245 planform.- The data for the 245 wing are found in figure 14(a) and table II(a). Low-damping periods could not be determined with any degree of certainty, because it was impossible to distinguish separate bending and torsion frequencies in the flutter records. This difficulty was due to the poor orientation of the strain gages on this wing, resulting in flutter records which showed only bending oscillations. Consequently, the data points represent only definite flutter points, but they do not necessarily identify the precise flutter boundary for this wing because of the difficulty in determining the exact start of flutter. All calculations of the reference flutter speeds were made with a two-mode analysis.

400 planform.- The data for the 400 wings are found in figure 14(b) and table II(b). Considerable difficulty was encountered in obtaining flutter on these wings because of a tendency toward static divergence. During the attempts to obtain flutter, several of these models diverged to destruction before fluttering. All calculations of the reference flutter speeds were made with a two-mode analysis.

430 planform.- The data for the 430 wings are found in figure 14(c) and table II(c). All calculations of the reference flutter speeds were made with a two-mode analysis.

445 planform.- The data for the 445 wings are found in figure 14(d) and table II(d). The calculations of the reference flutter speeds were made with a three-mode analysis.

452 planform.- The data for the 452 wings are found in figure 14(e) and table II(e). The calculations of the reference flutter speeds were made with a three-mode analysis.

460 planform.- The data for the 460 wings are found in figure 14(f) and table II(f). The flutter obtained on this planform in the subsonic speed range was very violent and frequently caused the compreg wings to crack within the fuselage block near the root. Ignorance of the existence of such a condition may explain the two points at  $M_e \approx 0.83$  which are below the curve in figure 14(f). The calculations of the reference flutter speeds were made with a three-mode analysis.

645 planform.- The data for the 645 wings are found in figure 14(g) and table II(g). The calculations of the reference flutter speeds were made with a three-mode analysis.

## DISCUSSION

### Effects of Sweep on the Flutter-Speed Ratio

The effects of sweepback angle on the variation of the flutter-speed ratio with Mach number are shown in figure 15 for wings with an aspect ratio of 4. This figure shows the faired curves of figure 14 for the appropriate planforms. Examination of figure 15 shows that  $V_e/V_R$  is near 1.0 for subsonic Mach numbers, that it increases with Mach number for supersonic Mach numbers, and that the effect of Mach number on  $V_e/V_R$  is considerably reduced for wings with large sweepback. The flutter-speed ratio increases as the sweepback angle is increased from  $0^\circ$  to  $30^\circ$ , but further increases in the sweepback angle from  $30^\circ$  to  $60^\circ$  result in a progressive reduction in the flutter-speed ratio to values which are near 1.0 throughout the Mach number range for the  $60^\circ$  sweptback planform. The curve of  $V_e/V_R$  for the unswept wings falls between the curves for the  $45^\circ$  sweptback wings and the  $52.5^\circ$  sweptback wings at supersonic Mach numbers. Difficulty was experienced in obtaining flutter on some of the models of the unswept wing because of a strong tendency toward static divergence. The possibility therefore exists that the flutter boundary of the wing may have been affected by the divergent tendencies.

### Effects of Aspect Ratio on the Flutter-Speed Ratio

The effects of aspect ratio on the variation of the flutter-speed ratio with Mach number are shown in figure 16 for wings with sweepback of  $45^\circ$ . This figure shows the faired curves of figure 14 for the appropriate planforms.

Figure 16 shows a large increase in flutter-speed ratio at the higher supersonic Mach numbers investigated as the aspect ratio is reduced from 6.4 to 4. It will be noted that a similar large increase in flutter-speed ratio is shown in the subsonic region as the aspect ratio is reduced from 4 to 2.4. The latter increase is probably due, at least in part, to inadequacies in the aerodynamic coefficients employed in the reference flutter-speed calculations, although other uncertainties arise in the attempt to treat the  $245$  wing as a simple beam.

### Effects of Additional Modes on the Reference Flutter Speed

The initial  $V_R$  calculations showed that for certain of the planforms the values of the reference flutter speeds obtained with two modes in the calculations tended to be too high and resulted in poor agreement between calculated and experimental flutter speeds. Consequently, calculations of the reference flutter speeds were made with three modes for the 445, 452, 460, and 645 planforms in an attempt to improve the agreement between  $V_e$  and  $V_R$ . A comparison of the flutter-speed ratios calculated with two modes and with three modes is shown in figures 17 to 20. In all cases, the addition of a third mode, the second uncoupled bending mode, is seen to result in reduced values of the reference flutter speeds and corresponding improvements in the agreement between  $V_e$  and  $V_R$  at subsonic Mach numbers. It will be noted from figures 17 to 20 and table I

that the effect of the addition of a third mode is related to the ratio of second bending to first torsion frequency. Within the range of the wings considered herein, the lower the second bending frequency with respect to the first torsion frequency, the greater the effect of the addition of a third mode. The addition of a third mode is seen to have relatively little effect in the case of the 445 wing. Since the ratios of second bending to first torsion frequency were even higher for the 400, 430, and 245 wings than for the 445 wing, only two modes were used in the analysis of these wings. The addition of a fourth mode, the third uncoupled bending mode, to the calculations for the 460 wing is seen in figure 19 to have little or no effect on the reference flutter speed.

#### Application of the Flutter-Speed Ratio

Caution should be exercised in applying the flutter-speed ratios to the determination of the flutter speed of wings which have values of  $\omega_{h,i}/\omega_\alpha$ ,  $x_\alpha$ ,  $a$ ,  $r_\alpha$ , and  $\mu$  much different from those which characterize the wings of the present investigation. It might be hoped that the reference flutter-speed calculations, as obtained in the present paper, have adequately removed from the results the effects of such variables as the center-of-gravity position, and that the curves of  $V_e/V_R$  against Mach number are a function of planform only. It is not evident, however, that such is the case.

#### Modified Experimental Flutter-Speed Coefficient

In order to provide some physical idea of the relationship between wing torsional frequency, flutter speed, and flutter mass-density ratio, figure 21 has been prepared. In this figure, an experimental flutter-speed coefficient corrected for mass-density ratio  $V_e/b_s\omega_\alpha\sqrt{\mu_e}$  is shown as a function of Mach number for all the planforms tested. The values of the experimental flutter-speed coefficient, its components, and the Mach numbers used to obtain the data points through which the faired curves of the figure were drawn were taken from tables I and II. It should be noted that curves of the parameter  $V_e/b_s\omega_\alpha\sqrt{\mu_e}$  against Mach number implicitly contain the effects of such important parameters as radius of gyration, center-of-gravity position, and frequency ratio. The data of figure 21 indicate, except for the 245 wing, a spread of about 30 percent in the parameter  $V_e/b_s\omega_\alpha\sqrt{\mu_e}$  at subsonic speeds with the 400 wing having the highest and the 460 wing the lowest values. For a given mass ratio, wing chord, and torsional frequency, the flutter-speed coefficients for the 245 wing are approximately twice as great as those of any of the other wings. In general, the variation of  $V_e/b_s\omega_\alpha\sqrt{\mu_e}$  with Mach number seems to be about the same as the variation of flutter-speed ratio  $V_e/V_R$  with Mach number. (See figs. 15 and 16.)

An interesting application of figure 21 may be seen if, for a given planform, the coefficient  $V_e/b_s\omega_\alpha\sqrt{\mu_e}$  is evaluated and plotted against Mach number for

values of  $V_e$ ,  $\mu_e$ , and  $M_e$  corresponding to flight conditions rather than flutter conditions. Some results of such an application are shown in figure 22, in which two example flight paths are shown in relation to the flutter boundary for the 445 planform. The straight-line flight path indicates the relation between velocity and Mach number for constant-altitude operation, the slope of the line being given by  $c/b_{S\alpha}\sqrt{\mu_e}$ . (The speed of sound corresponding to the given altitude is given by  $c$ .) The flight path indicated by the dashed line corresponds to a high-speed dive. Any intersections of these flight paths with the flutter boundary of the planform considered indicate a flutter condition. It should be noted that, for constant-altitude operation of a planform whose flutter boundary is characterized by a "knee," as at A in figure 22, the minimum altitude at which the wing will be flutter free throughout the Mach number range for which data are given is the altitude corresponding to the straight-line flight path which just misses the knee of the flutter boundary. For wings such as the 460, however, no knee exists in the flutter boundary shown in figure 21, at least within the scope of the data presented. Therefore, any constant-altitude path plotted for the 460 planform on figure 21 will intersect the 460 flutter boundary at some Mach number. If, for any of the planforms shown in figure 21, a high-speed dive is executed, an intersection with the flutter boundary may occur at the highest Mach numbers for which data are given, even for wings whose flutter boundaries are characterized by knees in the transonic range.

#### CONCLUSIONS

The results of an investigation of some of the effects of wing sweep and aspect ratio on the flutter characteristics of a series of thin cantilever wings at transonic speeds indicated the following conclusions:

1. The variation of flutter-speed ratio with Mach number was characterized, in most cases, by flutter-speed ratios near 1.0 at Mach numbers near 0.8, and an increase in flutter-speed ratio in the supersonic region up to Mach numbers near 1.4.
2. The rate of increase of the flutter-speed ratio with Mach number in the supersonic region increased as the sweep angle was increased from  $0^\circ$  to  $30^\circ$ , and then progressively decreased as the sweep angle was increased from  $30^\circ$  to  $60^\circ$ .
3. Reducing the aspect ratio from 6.4 to 2.4 resulted in progressively larger values of the flutter-speed ratio throughout the Mach number range of this investigation.

4. The use of the second uncoupled bending mode in addition to the uncoupled first bending and torsion modes in the reference flutter-speed calculations resulted, in many cases, in better agreement between the calculated and experimental flutter speeds at subsonic Mach numbers.

Langley Aeronautical Laboratory,  
National Advisory Committee for Aeronautics,  
Langley Field, Va., September 9, 1955.

#### REFERENCES

1. Bursnall, William J.: Initial Flutter Tests in the Langley Transonic Blowdown Tunnel and Comparison With Free-Flight Flutter Results. NACA RM L52K14, 1953.
2. Land, Norman S., and Abbott, Frank T., Jr.: Method of Controlling Stiffness Properties of a Solid-Construction Model Wing. NACA TN 3423, 1955.
3. Barmby, J. G., Cunningham, H. J., and Garrick, I. E.: Study of Effects of Sweep on the Flutter of Cantilever Wings. NACA Rep. 1014, 1951. (Supersedes NACA TN 2121.)

TABLE I.- PHYSICAL PROPERTIES OF MODELS

(a) 245 Planform

Parameter	Model 1
NACA section	65A004
A	2.4
$\Lambda$ , deg	45
$\lambda$	0.6
$\lambda_p$	0.685
Span, ft	0.808
$A_g$	0.91
$l$ , ft	0.306
$b_r$ , ft	0.129
$b_s$ , ft	0.183
$\xi_h$	0.023

$\eta$	Model 1				
	$x_\alpha$	a	$r_\alpha^2$	m, slugs/ft	$\theta$
0.05	-0.64	0.53	0.66	0.00217	0.98425
.15	-.66	.55	.69	.00207	.95275
.25	-.68	.57	.72	.00198	.92125
.35	-.70	.59	.74	.00189	.88975
.45	-.72	.61	.77	.00179	.85825
.55	-.74	.63	.80	.00170	.82675
.65	-.76	.65	.83	.00161	.79525
.75	-.78	.67	.86	.00152	.76375
.85	-.80	.69	.89	.00143	.73225
.95	-.82	.71	.92	.00134	.70175

Frequency	Model 1
	Left and right
$f_{h,1}$ , cps	135
$f_{h,2}$ , cps	630
$f_t$ , cps	425
$f_{b,1}$ , cps	149
$f_{b,2}$ , cps	519
$f_\alpha$ , cps	265
$(\omega_{b,1}/\omega_\alpha)^2$	0.3161
$(\omega_{b,2}/\omega_\alpha)^2$	3.836

TABLE I.- PHYSICAL PROPERTIES OF MODELS - Continued

(b) 400 Planform

Parameter	Models 1 and 2	Model 2					
		$\eta$	$x_\alpha$	a	$r_\alpha^2$	m, slugs/ft	$\theta$
NACA section	65A004						
A	4						
$\Lambda$ , deg	0						
$\lambda$	0.6	0.05	0.14	-0.23	0.24	0.00738	0.98285
$\lambda_p$	0.657	.15	.12	-.22	.25	.00716	.94855
Span, ft	1.142	.25	.11	-.21	.26	.00671	.91425
$A_g$	1.65	.35	.09	-.19	.27	.00617	.87995
$l$ , ft	0.445	.45	.08	-.18	.28	.00563	.84565
$b_r$ , ft	0.163	.55	.06	-.16	.28	.00509	.81135
$b_s$ , ft	0.163	.65	.05	-.15	.28	.00455	.77705
$g_h$	0.02	.75	.03	-.13	.27	.00400	.74275
		.85	.02	-.11	.25	.00345	.70845
		.95	.004	-.10	.24	.00291	.67415

Frequency	Model 1	Model 2	
	Left and right	Left	Right
$f_{h,1}$ , cps	147	147	154
$f_{h,2}$ , cps	630	680	725
$f_t$ , cps	407	390	404
$f_\alpha$ , cps	402	385	399
$(\omega_{h,1}/\omega_\alpha)^2$	0.133	0.146	0.149
$(\omega_{h,2}/\omega_\alpha)^2$	2.456	3.120	3.295

TABLE I.- PHYSICAL PROPERTIES OF MODELS - Continued

(c) 430 Platform

Parameter	Models 1, 2, 3, 4, and 5	
	65A004	
NACA section	4	
$\Delta$ , deg	30	
$\lambda$	0.6	
$\lambda_p$	0.657	
Span, ft	1.142	
$A_g$	1.65	
$l$ , ft	0.515	
$b_r$ , ft	0.149	
$b_s$ , ft	0.163	
$g_h$	0.036	

Frequency	Model 1		Model 2		Model 3		Model 4		Model 5	
	Left	Right								
$f_{h,1}$ , cps	107	108	102	98	103	102	102	98	102	103
$f_{h,2}$ , cps	501	499	508	470	525	520	510	510	470	480
$f_t$ , cps	350	339	370	340	342	350	328	342	350	340
$f_{\alpha}$ , cps	349	338	369	339	341	349	327	341	349	339
$(\omega_{h,1}/\omega_{\alpha})^2$	0.0939	0.1020	0.0763	0.0834	0.0911	0.0853	0.0971	0.0825	0.0853	0.0922
$(\omega_{h,2}/\omega_{\alpha})^2$	2.0607	2.1795	1.8953	1.9221	2.3704	2.2201	2.4324	2.2368	1.8136	2.0048

$\eta$	Model 1 (right)				
	$x_{\alpha}$	$a$	$r_{\alpha}^2$	$m$ , slugs/ft	$\theta$
0.05	0.09	-0.16	0.22	0.00864	0.98285
.15	.08	-.15	.23	.00781	.94855
.25	.07	-.14	.23	.00718	.91425
.35	.05	-.12	.23	.00658	.87995
.45	.04	-.11	.24	.00602	.84565
.55	.02	-.10	.24	.00554	.81135
.65	.01	-.08	.24	.00510	.77705
.75	-.002	-.07	.24	.00470	.74275
.85	-.02	-.06	.24	.00432	.70845
.95	-.03	-.04	.22	.00394	.67415

TABLE I.-- PHYSICAL PROPERTIES OF MODELS - Continued

(d) 445 Planform

Parameter	Models 1, 2, and 3	Model 1				Model 2				$\theta$
		$x_\alpha$	a	$r_\alpha^2$	m, slugs/ft	$x_\alpha$	a	$r_\alpha^2$	m, slugs/ft	
NACA section	65A004	0.05	-0.02	0.22	0.00561	0.037	-0.117	0.233	0.00733	0.98285
A	45	.15	.01	.22	.00527	.030	-.110	.234	.00648	.94855
$\Lambda$ , deg	0.6	.25	.04	.23	.00493	.023	-.102	.235	.00576	.91425
$\lambda$	0.657	.35	.07	.24	.00458	.016	-.095	.236	.00516	.87995
Span, ft	1.142	.45	.09	.24	.00424	.009	-.088	.237	.00472	.84565
$A_g$	1.65	.55	.12	.25	.00389	.002	-.082	.238	.00435	.81135
l, ft	0.630	.65	.15	.26	.00355	-.005	-.074	.239	.00407	.77705
$b_r$ , ft	0.123	.75	.17	.26	.00321	-.012	-.067	.240	.00382	.74275
$b_s$ , ft	0.163	.85	.20	.27	.00286	-.018	-.060	.241	.00361	.70855
$g_h$	0.030	.95	.23	.28	.00252	-.025	-.053	.242	.00343	.67415

Frequency	Model 1		Model 2		Model 3	
	Left and right	Left	Right	Left	Right	Right
$f_{h,1}$ , cps	88	67	64	78	73	
$f_{h,2}$ , cps	462	357	367	399	387	
$f_t$ , cps	370	356	342	389	378	
$f_\omega$ , cps	361	356	342	389	378	
$(\omega_{h,1}/\omega_\alpha)^2$	0.0594	0.0354	0.0350	0.0402	0.0373	
$(\omega_{h,2}/\omega_\alpha)^2$	1.638	1.006	1.151	1.053	1.049	

TABLE I.- PHYSICAL PROPERTIES OF MODELS - Continued

(e) 452 Planform

Parameter	Model 1	Model 1					
		$\eta$	$x_\alpha$	a	$r_\alpha^2$	m, slugs/ft	$\theta$
NACA section	65A004						
A	4						
$\Lambda$ , deg	52.5						
$\lambda$	0.6						
$\lambda_p$	0.657						
Span, ft	1.142						
$A_g$	1.65						
l, ft	0.732	0.05	0.37	-0.44	0.27	0.00573	0.98285
$b_r$ , ft	0.107	.15	.30	-.37	.27	.00538	.94855
$b_s$ , ft	0.163	.25	.24	-.31	.29	.00503	.91425
$\xi_h$	0.021	.35	.17	-.24	.32	.00468	.87995
		.45	.11	-.18	.29	.00433	.84565
		.55	.04	-.11	.27	.00398	.81135
		.65	-.02	-.05	.27	.00363	.77705
		.75	-.09	.02	.28	.00328	.74275
		.85	-.15	.08	.30	.00293	.70845
		.95	-.22	.15	.31	.00258	.67415

Frequency	Model 1
	Left and right
$f_{h,1}$ , cps	61
$f_{h,2}$ , cps	300
$f_t$ , cps	370
$f_\alpha$ , cps	366
$(\omega_{h,1}/\omega_\alpha)^2$	0.0282
$(\omega_{h,2}/\omega_\alpha)^2$	0.6717

TABLE I.- PHYSICAL PROPERTIES OF MODELS - Continued

(f) 460 Platform

Parameter	Models 1, 2, 3, 4, and 5		Models 1, 2, 3, and 4					Model 5					$\theta$
	65A004	4	$x_\alpha$	a	$r_\alpha^2$	m, slugs/ft	$x_\alpha$	a	$r_\alpha^2$	m, slugs/ft	$x_\alpha$	a	
NACA section	65A004		0.05	-0.31	0.26	0.00465	-0.136	0.040	0.230	0.00730	0.98285		
A	60		.15	-.23	.24	.00438	-.144	.048	.231	.00668	.94855		
$\Lambda$ , deg	0.6		.25	-.16	.23	.00410	-.152	.056	.234	.00612	.91425		
$\lambda$	0.657		.35	-.09	.23	.00383	-.160	.063	.237	.00562	.87995		
$\lambda_p$	1.142		.45	-.08	.24	.00356	-.167	.071	.246	.00518	.84565		
Span, ft	1.65		.55	-.15	.27	.00334	-.175	.079	.257	.00479	.81135		
Ag	0.892		.65	-.22	.30	.00320	-.183	.087	.252	.00442	.77705		
l, ft	0.086		.75	-.29	.19	.00314	-.191	.095	.242	.00400	.74275		
b <sub>r</sub> , ft	0.163		.85	-.36	.43	.00301	-.199	.103	.235	.00355	.70845		
b <sub>s</sub> , ft	0.163		.95	-.43	.51	.00283	-.207	.110	.232	.00305	.67415		
$\delta_h$	0.027												

Frequency	Model 1		Model 2		Model 3		Model 4		Model 5	
	Left	Right								
$f_{h,1}$ , cps	34.5	34.9	39.5	39.5	39	43.5	41	43	36.5	37.8
$f_{h,2}$ , cps	178	195	193	189	202	210	205	225	175	178
$f_{h,3}$ , cps	-----	510	-----	-----	-----	-----	-----	-----	425	410
$f_t$ , cps	363	370	430	390	390	421	430	435	452	480
$f_\alpha$ , cps	355	362	421	382	382	412	421	426	423	449
$(\omega_{h,1}/\omega_\alpha)^2$	0.0094	0.0093	0.0088	0.0107	0.0104	0.0111	0.0095	0.0102	0.0065	0.0062
$(\omega_{h,2}/\omega_\alpha)^2$	0.2514	0.2901	0.2101	0.2447	0.2795	0.2598	0.2371	0.2789	0.1063	0.1376
$(\omega_{h,3}/\omega_\alpha)^2$	-----	1.984	-----	-----	-----	-----	-----	-----	0.8845	0.7299

TABLE I.- PHYSICAL PROPERTIES OF MODELS - Concluded

(g) 645 Planform

Parameter	Model 1	Model 1				$\theta$	
		$\eta$	$x_\alpha$	a	$r_\alpha^2$		m, slugs/ft
NACA section	65A004						
A	6.4						
$\Lambda$ , deg	45						
$\lambda$	0.6	0.05	0.15	-0.25	0.26	0.00480	0.98230
$\lambda_p$	0.646	.15	.15	-.24	.26	.00437	.94690
Span, ft	1.400	.25	.14	-.23	.25	.00404	.91150
$A_g$	2.75	.35	.13	-.23	.25	.00381	.87610
$l$ , ft	0.813	.45	.13	-.22	.24	.00362	.84070
$b_r$ , ft	0.094	.55	.12	-.21	.24	.00335	.80530
$b_s$ , ft	0.127	.65	.11	-.21	.24	.00302	.76990
$\xi_h$	0.013	.75	.11	-.20	.25	.00266	.73450
		.85	.10	-.20	.28	.00243	.69910
		.95	.10	-.19	.33	.00226	.66370

Frequency	Model 1
	Left and right
$f_{h,1}$ , cps	46
$f_{h,2}$ , cps	227
$f_t$ , cps	522
$f_\alpha$ , cps	505
$(\omega_{h,1}/\omega_\alpha)^2$	0.0083
$(\omega_{h,2}/\omega_\alpha)^2$	0.2021

TABLE II.- COMPILATION OF ANALYTICAL AND TEST RESULTS

Wing panel behavior code: F - flutter E - end of flutter (dynamic pressure increasing)

N - no flutter G - strain gages inoperative

D - low damping X - wing panel destroyed or not installed

Subscripts: 1 - associated with first occurrence 2 - associated with second occurrence of flutter during the run

(a) 245 Planform

Model	Run *	Point †	Wing panel behavior		M <sub>e</sub>	V <sub>e</sub> /V <sub>R</sub>	ρ <sub>e</sub> , slugs/cu ft	μ <sub>e</sub>	√μ <sub>e</sub>	ω <sub>w</sub> , radians/sec	ω <sub>R</sub> , radians/sec	ω <sub>e</sub> , radians/sec	ω <sub>e</sub> /ω <sub>R</sub>	V <sub>e</sub> , ft/sec	V <sub>R</sub> , ft/sec	V <sub>e</sub> /V <sub>R</sub>	V <sub>e</sub> , lb/sq ft	V <sub>e</sub> /b <sub>1</sub> <sup>2</sup> ω <sub>e</sub>	V <sub>e</sub> /b <sub>1</sub> <sup>2</sup> ω <sub>R</sub>	V <sub>e</sub> /b <sub>1</sub> <sup>2</sup> ω <sub>e</sub> √μ <sub>e</sub>
			Left	Right																
1	1	1	F <sub>1</sub>	G	0.887	1.311	0.0041	12.13	3.48	1,665	1.180	1,965	1,684	0.857	896.0	683.7	4.17	3.18	1,646	0.8450
1	2	1	F <sub>1</sub>	F <sub>1</sub>	.980	1.477	.0047	10.65	3.26	1,665	1.198	1,995	1,797	.901	958.6	648.8	4.46	3.02	2,159	.9651
1	3	1	F <sub>1</sub>	F <sub>1</sub>	1.138	1.567	.0039	12.80	3.58	1,665	1.170	1,948	1,847	.948	1,092.7	697.1	5.09	3.25	2,328	1.0017
1	4	1	F <sub>1</sub>	F <sub>1</sub>	1.139	1.447	.0031	16.15	4.02	1,665	1.133	1,886	1,753	.929	1,101.3	761.2	5.13	3.54	1,862	.8991
1	5	1	F <sub>1</sub>	N	1.186	1.558	.0035	14.15	3.76	1,665	1.153	1,920	1,860	.969	1,131.7	726.6	5.27	3.38	2,241	.9878
1	6	1	F <sub>1</sub>	N	1.226	1.601	.0035	14.44	3.80	1,665	1.153	1,920	1,954	1.018	1,163.1	726.6	5.42	3.38	2,367	1.0045
1	7	1	F <sub>1</sub>	N	1.302	1.666	.0035	14.15	3.76	1,665	1.153	1,920	1,973	1.028	1,210.7	726.6	5.64	3.38	2,565	1.0568
1	8	1	F <sub>1</sub>	F <sub>1</sub>	1.308	1.732	.0039	12.94	3.60	1,665	1.170	1,948	1,923	.987	1,207.7	697.1	5.62	3.25	2,844	1.1010
1	9	1	F <sub>1</sub>	F <sub>1</sub>	1.267	1.673	.0038	13.02	3.61	1,665	1.168	1,945	2,004	1.030	1,177.2	703.8	5.48	3.28	2,633	1.0702
1	10	1	F <sub>1</sub>	F <sub>1</sub>	.924	1.333	.0039	12.68	3.56	1,665	1.170	1,948	1,766	.907	929.2	697.1	4.33	3.25	1,655	.8566
1	11	1	F <sub>1</sub>	X	1.099	1.446	.0033	14.98	3.87	1,665	1.145	1,906	1,784	.936	1,074.7	743.3	5.00	3.46	1,906	.9114
1	12	1	F <sub>1</sub>	F <sub>1</sub>	1.099	1.391	.0029	17.32	4.16	1,665	1.123	1,870	1,552	.830	1,085.5	780.6	5.05	3.63	1,708	.8564

\* A run is defined as one operation of the blowdown tunnel from valve opening to valve closing.

† Chronological order in which recorded points occurred during the test run.

TABLE II.- COMPILATION OF ANALYTICAL AND TEST RESULTS - Continued

(b) 400 Planform

Model	Run*	Point †	Wing panel behavior		Me	Ve/V <sub>R</sub>	ρ <sub>e</sub> slugs cu ft	μ <sub>e</sub>	√μ <sub>e</sub>	ω <sub>ω</sub> radians sec	ω <sub>R</sub> /ω <sub>ω</sub>	ω <sub>R</sub> radians sec	ω <sub>e</sub> radians sec	ω <sub>e</sub> /ω <sub>R</sub>	V <sub>e</sub> ft/sec	V <sub>R</sub> ft/sec	V <sub>e</sub> b <sub>ω</sub> /ω <sub>ω</sub>	V <sub>R</sub> b <sub>ω</sub> /ω <sub>ω</sub>	q <sub>e</sub> lb/sq ft	V <sub>e</sub> b <sub>ω</sub> ω <sub>ω</sub> /μ <sub>e</sub>
			Left	Right																
1	1	1	N	D <sub>1</sub>	0.890	0.961	0.0031	28.32	5.32	2,526	-----	-----	-----	-----	877.0	914.1	2.133	2.22	1,184.4	0.3547
1	1	2	N	F <sub>1</sub>	.919	.997	.0031	28.06	5.30	2,526	0.3550	896.7	1.058	1.180	902.9	905.8	2.192	2.20	1,263.1	.4138
1	2	1	N	D <sub>1</sub>	.886	.970	.0031	27.89	5.28	2,526	-----	-----	-----	-----	874.8	901.7	2.125	2.19	1,193.2	.4024
1	2	2	N	F <sub>1</sub>	.908	.991	.0032	27.44	5.24	2,526	.3480	879.0	1.062	1.208	889.3	897.6	2.159	2.18	1,253.1	.4122
1	3	1	N	D <sub>1</sub>	.917	.956	.0028	30.77	5.55	2,526	-----	-----	-----	-----	901.1	942.9	2.189	2.29	1,147.4	.3943
1	3	2	N	F <sub>1</sub>	.986	1.021	.0028	30.58	5.53	2,526	.3628	916.4	-----	-----	958.3	938.7	2.327	2.28	1,305.8	.4209
1	4	1	N	D <sub>1</sub>	.955	.973	.0027	32.21	5.68	2,526	-----	-----	-----	-----	941.2	967.6	2.290	2.33	1,196.0	.4024
1	4	2	N	F <sub>1</sub>	.949	.990	.0029	30.36	5.51	2,526	.3725	940.9	1.070	1.137	933.8	942.9	2.268	2.29	1,264.4	.4116
1	5	1	D <sub>1</sub>	N	.984	.948	.0024	36.24	6.02	2,526	-----	-----	-----	-----	968.3	1,021.1	2.350	2.45	1,125.0	.3906
1	5	2	F <sub>1</sub>	N	1.027	.991	.0025	35.13	5.93	2,526	.4002	1,010.9	1.057	1.046	1,000.0	1,008.8	2.429	2.45	1,250.0	.4096
1	6	1	N	D <sub>1</sub>	1.336	1.270	.0028	31.02	5.57	2,526	-----	-----	-----	-----	1,208.0	951.1	2.934	2.31	2,043.0	.5287
1	6	2	D <sub>1</sub>	F <sub>1</sub>	1.333	1.340	.0032	27.14	5.21	2,526	-----	-----	-----	-----	1,197.2	893.5	2.908	2.17	2,293.3	.5581
1	6	3	D <sub>1</sub>	F <sub>1</sub>	1.338	1.335	.0032	27.30	5.22	2,526	.3533	892.4	1.416	1.587	1,198.7	897.6	2.911	2.18	2,299.0	.5577
1	6	4	F <sub>1</sub>	F <sub>1</sub>	1.318	1.370	.0035	24.92	4.99	2,526	.3378	853.3	1.375	1.611	1,179.0	860.5	2.863	2.09	2,432.6	.5738
1	7	1	D <sub>1</sub>	D <sub>1</sub>	.941	.938	.0026	33.39	5.78	2,526	-----	-----	-----	-----	923.0	984.1	2.242	2.39	1,107.5	.3878
1	7	2	F <sub>1</sub>	F <sub>1</sub>	1.051	1.025	.0026	33.41	5.78	2,526	.3903	985.9	1.414	1.434	1,008.7	984.1	2.450	2.39	1,322.7	.4238
1	7	3	D <sub>1</sub>	F <sub>1</sub>	1.154	1.121	.0027	32.17	5.67	2,526	-----	-----	-----	-----	1,085.0	967.6	2.635	2.35	1,589.3	.4648
1	7	4	D <sub>1</sub>	F <sub>2</sub>	1.227	1.253	.0032	27.15	5.21	2,526	.3527	890.9	1.257	1.411	1,119.3	893.5	2.718	2.17	2,004.5	.5218
1	8	1	D <sub>1</sub>	D <sub>1</sub>	1.034	1.015	.0025	34.75	5.89	2,526	-----	-----	-----	-----	1,015.6	1,000.5	2.467	2.35	1,289.3	.4188
1	8	2	D <sub>1</sub>	F <sub>1</sub>	1.100	1.081	.0026	33.45	5.78	2,526	.3902	985.6	1.204	1.222	1,063.5	984.1	2.583	2.49	1,470.3	.4469
1	8	3	F <sub>1</sub>	F <sub>1</sub>	1.227	1.255	.0030	28.99	5.38	2,526	-----	-----	-----	-----	1,152.8	918.2	2.800	2.23	1,993.4	.5217
1	9	1	F <sub>1</sub>	N	1.009	1.039	.0029	30.16	5.49	2,526	.3710	937.1	1.126	1.202	975.5	938.8	2.369	2.28	1,379.8	.4316
1	10	1	F <sub>1</sub>	N	.950	.979	.0028	31.10	5.58	2,526	.3770	952.3	1.100	1.155	934.1	951.1	2.262	2.31	1,214.5	.4066
1	11	1	D <sub>1</sub>	N	.878	.978	.0033	26.32	5.13	2,526	-----	-----	-----	-----	861.7	881.1	2.093	2.14	1,225.2	.4080
1	11	2	F <sub>1</sub>	N	.926	1.031	.0034	25.52	5.05	2,526	.3418	863.4	1.156	1.339	899.8	872.9	2.185	2.12	1,376.4	.4327
1	12	1	D <sub>1</sub>	X	.863	.912	.0028	31.02	5.57	2,526	-----	-----	-----	-----	867.5	951.1	2.107	2.31	1,053.6	.3783
1	12	2	F <sub>1</sub>	X	.949	.990	.0029	29.82	5.46	2,526	.3692	932.6	1.112	1.192	925.7	934.6	2.248	2.27	1,242.5	.4118
1	13	1	F <sub>1</sub>	X	1.017	1.014	.0026	33.33	5.77	2,526	.3898	984.6	1.125	1.142	993.3	979.9	2.412	2.38	1,282.6	.4181
1	14	1	D <sub>1</sub>	X	.930	.948	.0027	32.17	5.67	2,526	-----	-----	-----	-----	917.3	967.6	2.228	2.35	1,135.9	.3929
1	14	2	F <sub>1</sub>	X	1.017	1.008	.0027	32.66	5.71	2,526	.3855	973.8	1.125	1.155	983.2	975.8	2.368	2.37	1,305.0	.4182
1	15	1	D <sub>1</sub>	X	1.284	1.324	.0034	25.58	5.06	2,526	-----	-----	-----	-----	1,156.1	872.9	2.808	2.12	2,272.2	.5549
1	15	2	F <sub>1</sub>	X	1.259	1.391	.0039	22.30	4.72	2,526	.3200	808.3	1.423	1.760	1,134.1	815.2	2.754	1.98	2,508.1	.5836
1	16	1	F <sub>1</sub>	X	.988	.963	.0026	32.86	5.73	2,526	.3870	977.6	1.145	1.171	958.9	975.8	2.329	2.37	1,195.3	.4064
1	16	2	D <sub>2</sub>	X	1.267	1.260	.0030	28.95	5.38	2,526	-----	-----	-----	-----	1,161.8	922.3	2.822	2.24	2,024.7	.5245
1	16	3	F <sub>2</sub>	X	1.262	1.280	.0031	27.66	5.26	2,526	.3560	899.3	1.348	1.499	1,154.0	901.7	2.803	2.19	2,064.2	.5328
1	17	1	F <sub>1</sub>	X	1.052	1.014	.0025	34.43	5.87	2,526	.3960	1,000.3	1.149	1.149	1,014.4	1,000.5	2.464	2.43	1,286.3	.4197
1	18	1	D <sub>1</sub>	X	1.348	1.420	.0036	24.13	4.91	2,526	-----	-----	-----	-----	1,204.2	848.2	2.925	2.06	2,610.2	.5956
1	18	2	F <sub>1</sub>	X	1.328	1.471	.0040	21.74	4.66	2,526	.3160	798.2	1.494	1.872	1,187.4	807.0	2.884	1.96	2,819.8	.6188
1	19	1	D <sub>1</sub>	X	1.411	1.387	.0029	29.95	5.47	2,526	-----	-----	-----	-----	1,296.7	934.6	3.149	2.27	2,438.1	.5757
1	19	2	F <sub>1</sub>	X	1.383	1.444	.0033	26.36	5.13	2,526	.3475	877.8	1.466	1.670	1,272.5	881.1	3.091	2.14	2,671.8	.6024
2	20	1	F <sub>1</sub>	X	.920	1.001	.0025	35.45	5.95	2,422	.4015	972.4	1,112	1.144	971.2	970.6	2.460	2.46	1,179.0	.4134
2	21	1	F <sub>1</sub>	X	.943	.996	.0024	36.74	6.06	2,422	.4090	990.6	1,081	1.091	982.7	986.4	2.489	2.50	1,158.8	.4108
2	22	1	D <sub>1</sub>	X	1.032	1.004	.0021	42.34	6.51	2,422	.4388	1,062.8	1,125	1.059	1,058.1	1,053.4	2.680	2.67	1,175.8	.4117
2	22	2	F <sub>1</sub>	X	1.145	1.079	.0020	43.40	6.59	2,422	.4440	1,075.4	1,125	1.046	1,149.2	1,065.3	2.911	2.70	1,320.7	.4417
2	23	1	D <sub>1</sub>	X	1.050	1.024	.0021	41.81	6.47	2,422	-----	-----	-----	-----	1,070.2	1,045.5	2.711	2.65	1,202.6	.4190
2	23	2	F <sub>1</sub>	X	1.105	1.059	.0021	42.34	6.51	2,422	.4388	1,062.8	1,106	1.041	1,115.6	1,053.4	2.826	2.67	1,306.8	.4341
2	24	1	D <sub>1</sub>	X	.875	.976	.0026	33.50	5.79	2,422	-----	-----	-----	-----	920.1	943.0	2.331	2.39	1,100.6	.4025
2	24	2	F <sub>1</sub>	X	.904	1.006	.0026	33.13	5.76	2,422	.3890	942.2	1,081	1.147	945.0	939.0	2.394	2.38	1,160.9	.4156
2	25	1	F <sub>1</sub>	X	.865	1.013	.0029	30.10	5.49	2,422	.3708	898.1	1.175	1.308	907.3	895.6	2.298	2.27	1,193.6	.4186
2	26	1	F <sub>1</sub>	X	1.301	1.282	.0024	36.59	6.05	2,422	.4080	988.2	1.262	1.297	1,259.6	982.4	3.191	2.49	1,903.9	.5274
3	27	1	N	D <sub>1</sub>	1.333	1.426	.0029	29.98	5.48	2,422	-----	-----	-----	-----	1,277.1	895.6	3.235	2.27	2,364.9	.5903
3	27	2	N	F <sub>1</sub>	1.328	1.476	.0032	27.48	5.24	2,422	.3545	858.6	1.319	1.536	1,269.7	860.1	3.216	2.18	2,579.4	.6138

\*A run is defined as one operation of the blowdown tunnel from valve opening to valve closing.  
†Chronological order in which recorded points occurred during the test run.

TABLE II.- COMPILATION OF ANALYTICAL AND TEST RESULTS - Continued

(c) 430 Planform

Model	Run*	Point†	Wing panel behavior		M <sub>∞</sub>	V <sub>∞</sub> /V <sub>R</sub>	ρ <sub>e</sub> <sup>1</sup> slugs cu ft	Re	√μ <sub>e</sub>	ω <sub>α</sub> radians sec	ω <sub>R</sub> /ω <sub>α</sub>	ω <sub>R</sub> radians sec	ω <sub>e</sub> radians sec	ω <sub>e</sub> /ω <sub>R</sub>	V <sub>e</sub> <sup>1</sup> ft/sec	V <sub>R</sub> ft/sec	V <sub>e</sub> b <sub>1</sub> /ω <sub>α</sub>	V <sub>R</sub> b <sub>2</sub> /ω <sub>α</sub>	Q <sub>e</sub> <sup>1</sup> lb/sq ft	V <sub>e</sub> b <sub>1</sub> /ω <sub>α</sub> √μ <sub>e</sub>
			Left	Right																
1	1	1	D <sub>1</sub>	D <sub>1</sub>	0.774	1.074	0.0030	40.07	6.33	2,159	-----	-----	-----	-----	816.4	759.8	2.538	2.362	1,000	0.3665
1	1	2	F <sub>1</sub>	F <sub>1</sub>	.796	1.121	.0032	38.17	6.18	2,159	0.5373	1,160	1,100	0.948	836.0	745.7	2.599	2.318	1,118	.3844
1	2	1	D <sub>1</sub>	D <sub>1</sub>	1.369	1.763	.0035	34.90	5.91	2,159	-----	-----	-----	1,268.5	719.6	3.945	2.237	2,816	.6099	
1	2	2	F <sub>1</sub>	F <sub>1</sub>	1.360	1.891	.0044	27.76	5.27	2,159	.5888	1,206	1,596	1.323	1,246.0	658.8	3.873	2.048	3,416	.6718
1	3	1	F <sub>1</sub>	F <sub>1</sub>	.899	1.140	.0025	48.86	6.99	2,159	.5188	1,120	993	.887	937.4	822.2	2.914	2.556	1,098	.3811
1	3	2	E <sub>1</sub>	E <sub>1</sub>	.963	1.199	.0025	48.86	6.99	2,159	.5188	1,120	-----	-----	986.1	822.2	3.065	2.556	1,215	.4009
1	3	3	D <sub>2</sub>	D <sub>2</sub>	1.168	1.553	.0032	38.17	6.18	2,159	-----	-----	-----	1,157.0	745.0	3.597	2.316	2,142	.5320	
1	3	4	F <sub>2</sub>	F <sub>2</sub>	1.158	1.623	.0037	33.01	5.74	2,159	.5478	1,183	1,433	1.211	1,142.9	704.2	3.553	2.189	2,416	.5658
1	4	1	F <sub>1</sub>	F <sub>1</sub>	.913	1.100	.0022	55.52	7.45	2,159	-----	-----	942	-----	952.4	866.0	2.961	2.692	998	.3633
1	4	2	E <sub>1</sub>	E <sub>1</sub>	.959	1.148	.0022	55.52	7.45	2,159	-----	-----	-----	-----	994.4	866.0	3.091	2.692	1,088	.3793
1	4	3	D <sub>2</sub>	D <sub>2</sub>	1.249	1.634	.0032	38.17	6.18	2,159	-----	-----	-----	1,217.4	745.0	3.784	2.316	2,371	.5598	
1	4	4	F <sub>2</sub>	F <sub>2</sub>	1.251	1.727	.0037	33.01	5.74	2,159	.5478	1,183	1,451	1.226	1,216.2	704.2	3.781	2.189	2,736	.6021
1	5	1	G	F <sub>1</sub>	.850	1.135	.0029	42.11	6.49	2,125	.5303	1,127	1,024	.909	865.1	762.4	2.732	2.408	1,085	.3848
1	5	2	G	E <sub>1</sub>	.884	1.172	.0029	42.11	6.49	2,125	.5303	1,127	-----	-----	893.4	762.4	2.822	2.408	1,157	.3974
2	6	1	F <sub>1</sub>	F <sub>1</sub>	.850	1.068	.0026	46.98	6.85	2,227	.5217	1,161.8	1,037	.892	894.0	834.9	2.694	2.516	1,039	.3595
2	7	1	F <sub>1</sub>	F <sub>1</sub>	.820	1.034	.0026	46.98	6.85	2,227	.5217	1,161.8	999	.960	863.0	834.9	2.601	2.516	968	.3471
2	8	1	F <sub>1</sub>	F <sub>1</sub>	.855	1.027	.0023	53.11	7.29	2,227	.5141	1,145	955	.834	900.3	877.0	2.713	2.643	932	.3261
2	8	2	E <sub>1</sub>	E <sub>1</sub>	.947	1.120	.0023	53.11	7.29	2,227	.5141	1,145	-----	-----	984.0	877.0	2.643	2.643	1,113	.3402
2	8	3	N	F <sub>2</sub>	1.227	1.669	.0034	35.93	5.99	2,131	.5418	1,154.6	1,433	1.241	1,199.0	718.2	3.776	2.262	2,444	.5763
2	8	4	D <sub>2</sub>	F <sub>2</sub>	1.219	1.620	.0041	29.79	5.46	2,319	-----	-----	-----	1,178.4	727.3	3.410	2.105	2,847	.5710	
2	8	5	F <sub>2</sub>	F <sub>2</sub>	1.235	1.732	.0049	24.93	4.99	2,319	.5656	1,311.6	1,571	1.198	1,177.6	680.0	3.408	1.968	3,398	.6243
2	9	1	F <sub>1</sub>	G	.833	.997	.0025	48.86	6.99	2,319	.5188	1,203.1	968	.804	884.0	883.2	2.558	2.556	977	.3346
2	9	2	F <sub>1</sub>	G	.994	1.192	.0027	45.24	6.73	2,319	.5246	1,217.0	-----	-----	1,024.0	855.9	2.964	2.477	1,416	.4025
2	9	3	D <sub>2</sub>	G	1.129	1.461	.0035	34.90	5.91	2,319	-----	-----	-----	1,129.3	773.0	3.268	2.237	2,232	.5055	
2	9	4	F <sub>2</sub>	G	1.130	1.544	.0041	29.79	5.46	2,319	.5543	1,285.4	1,458	1.134	1,123.4	727.3	3.251	2.105	2,587	.5443
2	10	1	F <sub>1</sub>	G	.848	1.012	.0025	48.86	6.99	2,319	.5186	1,203	999	.830	894	883.2	2.587	2.556	999	.3384
2	10	2	E <sub>1</sub>	G	.995	1.186	.0027	45.24	6.73	2,319	.5246	1,216	-----	-----	1,018	855.9	2.946	2.477	1,399	.4002
2	10	3	D <sub>2</sub>	G	1.088	1.353	.0031	39.40	6.28	2,319	-----	-----	-----	1,096	810.3	3.172	2.345	1,862	.4617	
2	10	4	F <sub>2</sub>	G	1.095	1.437	.0036	33.93	5.82	2,319	.5458	1,266	1,389	1.097	1,099	764.7	3.181	2.213	2,174	.4996
2	11	1	F <sub>1</sub>	F <sub>1</sub>	.814	1.035	.0026	46.98	6.85	2,227	.5217	1,162	1,005	.865	864	834.9	2.604	2.516	970	.3475
2	12	1	F <sub>1</sub>	X	.885	1.040	.0024	50.90	7.13	2,319	.5152	1,195	930	.778	934	896.0	2.703	2.599	1,047	.3466
2	12	2	E <sub>1</sub>	X	.930	1.086	.0024	50.90	7.13	2,319	.5152	1,195	-----	-----	975	896.0	2.822	2.599	1,141	.3618
2	12	3	D <sub>2</sub>	X	1.172	1.449	.0032	38.17	6.18	2,319	-----	-----	-----	1,160	800.6	3.357	2.317	2,153	.4966	
2	12	4	F <sub>2</sub>	X	1.161	1.533	.0038	32.14	5.67	2,319	.5493	1,274	1,363	1.070	1,147	748.4	3.320	2.166	2,500	.5352
3	13	1	D <sub>1</sub>	D <sub>1</sub>	.746	1.055	.0031	39.43	6.28	2,169	-----	-----	-----	800.0	758.2	2.475	2.346	992	.3603	
3	13	2	F <sub>1</sub>	F <sub>1</sub>	.750	1.081	.0034	35.95	6.00	2,169	.5416	1,175	1,068	.909	791.1	732.0	2.448	2.265	1,064	.3729
4	14	1	F <sub>1</sub>	F <sub>1</sub>	.780	1.045	.0026	46.97	6.85	2,100	.5216	1,095	1,056	.964	822.7	786.9	2.629	2.515	880	.3509
5	15	1	E <sub>1</sub>	D <sub>1</sub>	.785	1.118	.0034	35.95	6.00	2,159	-----	-----	-----	814.8	728.6	2.535	2.267	1,129	.3861	
5	15	2	F <sub>1</sub>	F <sub>1</sub>	.812	1.163	.0035	34.92	5.91	2,159	.5416	1,169.3	1,097	.938	837.5	719.9	2.603	2.238	1,227	.3966

\*A run is defined as one operation of the blowdown tunnel from valve opening to valve closing.

†Chronological order in which recorded points occurred during the test run.

TABLE II.- COMPILATION OF ANALYTICAL AND TEST RESULTS - Continued

(d) 445 Platform

Model	Run*	Point †	Wing panel behavior		M <sub>e</sub>	V <sub>e</sub> /V <sub>R</sub>	P <sub>e</sub> , slug/cu ft	μ <sub>e</sub>	W <sub>e</sub>	α <sub>w</sub> , radians/sec	α <sub>R</sub> /α <sub>w</sub>	α <sub>R</sub> , radians/sec	α <sub>e</sub> , radians/sec	α <sub>e</sub> /ω <sub>R</sub>	V <sub>e</sub> , ft/sec	V <sub>R</sub> , ft/sec	V <sub>e</sub> /V <sub>R</sub>	V <sub>R</sub> /V <sub>e</sub>	q <sub>e</sub> , lb/ft <sup>2</sup> sq	V <sub>e</sub> /b <sub>e</sub> α <sub>w</sub> W <sub>e</sub>
			Left	Right																
1	1	1	F <sub>1</sub>	F <sub>1</sub>	0.813	1.032	0.0033	37.10	6.09	2,268	0.5295	1,201.5	1,047	0.871	805.4	780.4	2.88	2.80	1,070	0.3577
1	2	1	F <sub>1</sub>	F <sub>1</sub>	.797	1.039	.0031	39.49	6.28	2,268	.5245	1,200.9	1,047	.872	795.6	765.8	2.85	2.75	981	.3427
1	3	1	F <sub>1</sub>	F <sub>1</sub>	.863	1.036	.0028	43.72	6.61	2,268	.5160	1,170.3	995	.850	856.0	825.8	3.06	2.96	1,026	.3503
1	4	1	F <sub>1</sub>	F <sub>1</sub>	.863	1.030	.0028	43.72	6.61	2,268	.5160	1,170.3	---	---	850.7	825.8	3.04	2.96	1,013	.3481
1	5	1	F <sub>1</sub>	F <sub>1</sub>	.906	1.047	.0026	47.08	6.86	2,268	.5095	1,155.5	995	.861	887.7	848.1	3.18	3.04	1,024	.3500
1	6	1	F <sub>1</sub>	F <sub>1</sub>	.904	1.062	.0027	45.34	6.73	2,268	.5128	1,163.0	958	.824	888.8	837.0	3.19	3.00	1,067	.3572
1	7	1	N	D <sub>1</sub>	1.396	1.987	.0029	42.21	6.50	2,268	.5192	1,177.5	---	---	1,296.7	817.4	4.65	2.93	2,439	.5396
1	7	2	N	F <sub>1</sub>	1.376	1.641	.0034	36.01	6.00	2,268	.5322	1,207.0	1,585	1.313	1,267.8	772.7	4.55	2.77	2,732	.5716
1	7	3	D <sub>1</sub>	F <sub>1</sub>	1.326	1.800	.0048	29.50	5.05	2,268	.5569	1,263.0	---	---	1,215.0	675.1	4.36	2.42	2,067	.6508
1	7	4	F <sub>1</sub>	F <sub>1</sub>	1.340	1.830	.0054	22.67	4.76	2,268	.5643	1,279.8	1,755	1.371	1,214.8	663.9	4.36	2.36	3,984	.6903
1	8	1	N	F <sub>1</sub>	1.023	1.095	.0021	59.73	7.73	2,268	.4870	1,104.5	1,119	1.013	1,011.0	923.0	3.62	3.32	1,073	.3538
1	8	2	N	F <sub>2</sub>	1.361	1.614	.0033	36.88	6.07	2,268	.5302	1,202.4	1,281	1.281	1,256.0	778.0	4.50	2.79	2,603	.5597
1	9	1	F <sub>1</sub>	F <sub>1</sub>	.975	1.124	.0024	51.23	7.16	2,268	.5016	1,137.6	1,121	.985	981.0	873.0	3.51	3.13	1,155	.3706
1	9	2	F <sub>1</sub>	E <sub>1</sub>	1.304	1.540	.0031	38.99	6.24	2,268	.5255	1,191.8	---	---	1,224.0	795.0	4.38	2.84	2,322	.5306
1	10	1	F <sub>1</sub>	F <sub>1</sub>	.975	1.125	.0025	49.77	7.05	2,268	.5047	1,144.6	1,023	.894	973.0	865.0	3.48	3.10	1,183	.3733
1	11	1	F <sub>1</sub>	F <sub>1</sub>	.924	1.052	.0026	47.08	6.86	2,268	.5095	1,155.5	1,040	.900	921.0	875.0	3.30	3.04	1,103	.3632
1	12	1	F <sub>1</sub>	F <sub>1</sub>	.794	.972	.0028	43.72	6.61	2,268	.5160	1,170.3	1,063	.908	803.3	825.8	2.88	2.96	903	.3287
1	13	1	N	F <sub>1</sub>	.961	1.065	.0022	55.64	7.46	2,268	.4938	1,120.0	1,096	.978	956.0	901.1	3.42	3.23	1,005	.3466
1	13	2	N	F <sub>2</sub>	1.342	1.600	.0035	34.98	5.92	2,268	.5342	1,212.0	1,570	1.295	1,223.0	764.4	4.38	2.74	2,618	.5588
2	14	1	N	F <sub>1</sub>	.940	1.059	.0018	80.93	9.00	2,149	.4019	863.6	859	.995	977.0	922.4	3.69	3.49	860	.3099
2	14	2	N	E <sub>1</sub>	1.039	1.129	.0017	85.69	9.26	2,149	---	---	---	---	1,062.0	940.9	4.01	3.56	952	.3274
2	15	1	N	F <sub>1</sub>	.862	1.007	.0019	76.67	8.76	2,149	.4078	876.3	856	.980	908.0	901.3	3.43	3.41	768	.2959
2	15	2	N	E <sub>1</sub>	1.049	1.140	.0017	85.69	9.26	2,149	---	---	---	---	1,073.0	940.9	4.06	3.56	1,004	.3308
2	16	1	F <sub>1</sub>	F <sub>1</sub>	.871	1.041	.0024	60.70	7.79	2,195	.4325	949.3	919	.968	882.0	847.5	3.27	3.14	922	.3164
2	16	2	G	E <sub>1</sub>	1.175	1.336	.0020	72.84	8.53	2,149	---	---	---	---	1,183.0	885.4	4.48	3.35	1,426	.3960
2	16	3	G	D <sub>2</sub>	1.293	1.705	.0037	39.37	6.27	2,149	.4713	1,012.7	---	---	1,217.0	713.6	4.60	2.70	2,753	.5542
2	16	4	G	F <sub>2</sub>	1.292	1.741	.0038	38.34	6.19	2,149	.4736	1,017.7	1,460	1.435	1,233.0	708.3	4.66	2.68	2,920	.5687
2	17	1	F <sub>1</sub>	G	.830	1.044	.0026	56.03	7.49	2,237	.4402	984.6	982	.997	879.0	841.9	3.19	3.06	996	.3219
3	18	1	D <sub>1</sub>	G	1.348	1.643	.0041	35.53	5.96	2,444	---	---	---	---	1,289.0	784.7	4.29	2.61	3,411	.5429
3	18	2	F <sub>1</sub>	G	1.346	1.712	.0049	29.73	5.45	2,444	.4925	1,203.8	1,591	1.322	1,271.0	742.6	4.23	2.47	3,979	.5854
3	19	1	D <sub>1</sub>	G	1.219	1.423	.0033	44.15	6.64	2,444	---	---	---	---	1,202.0	844.8	4.00	2.81	2,388	.4544
3	19	2	F <sub>1</sub>	G	1.192	1.445	.0037	39.37	6.27	2,444	.4712	1,151.7	1,302	1.130	1,173.0	811.7	3.90	2.70	2,537	.4696
3	20	1	D <sub>1</sub>	G	1.204	1.411	.0033	44.15	6.64	2,444	---	---	---	---	1,192.0	844.8	3.96	2.81	2,328	.4506
3	20	2	F <sub>1</sub>	G	1.186	1.464	.0039	37.35	6.11	2,444	.4756	1,162.4	1,353	1.164	1,166.0	804.4	3.88	2.68	2,628	.4790
3	21	1	F <sub>1</sub>	G	.836	1.063	.0025	58.27	7.63	2,444	.4369	1,067.9	900	.843	997.0	929.0	3.32	3.09	1,104	.3280
3	22	1	N	D <sub>1</sub>	1.307	1.600	.0037	39.37	6.27	2,375	.4713	1,119.3	---	---	1,262.0	788.8	4.32	2.70	2,946	.5199
3	22	2	N	F <sub>1</sub>	1.332	1.682	.0044	33.11	5.75	2,375	.4848	1,151.4	1,539	1.337	1,253.1	744.9	4.29	2.55	3,454	.5629
3	23	1	F <sub>1</sub>	F <sub>1</sub>	.882	.980	.0022	66.22	8.14	2,410	.4237	1,021.1	905	.886	939.8	960.0	3.17	3.24	971	.2939
3	23	2	E <sub>1</sub>	E <sub>1</sub>	1.149	1.183	.0020	72.84	8.53	2,410	---	---	---	---	1,173.9	993.0	3.96	3.35	1,378	.3503
3	23	3	N	D <sub>2</sub>	1.285	1.528	.0033	44.15	6.64	2,375	.4618	1,096.8	---	---	1,254.0	820.9	4.29	2.81	2,595	.4878
3	23	4	N	F <sub>2</sub>	1.283	1.591	.0038	38.34	6.19	2,375	.4736	1,124.8	1,495	1.329	1,245.8	782.9	4.26	2.68	2,949	.5199
3	24	1	F <sub>1</sub>	F <sub>1</sub>	.854	1.037	.0028	52.03	7.21	2,410	.4475	1,078.5	955	.885	912.8	880.0	3.08	2.97	1,166	.3223
3	25	1	F <sub>1</sub>	F <sub>1</sub>	.908	1.033	.0024	60.70	7.79	2,410	.4326	1,142.6	930	.892	961.3	931.0	3.24	3.14	1,109	.3141
3	25	2	E <sub>1</sub>	G	1.085	1.184	.0023	63.34	7.96	2,410	---	---	---	---	1,116.1	943.0	3.76	3.18	1,432	.3569
3	25	3	D <sub>2</sub>	G	1.142	1.242	.0026	56.03	7.49	2,444	.4402	1,075.9	---	---	1,142.3	920.0	3.80	3.06	1,696	.3282
3	25	4	F <sub>2</sub>	G	1.176	1.306	.0028	52.03	7.21	2,444	.4475	1,093.8	1,115	1.019	1,166.4	892.9	3.88	2.97	1,905	.4060
3	26	1	F <sub>1</sub>	G	.874	.997	.0025	58.27	7.63	2,444	.4367	1,067.4	892	.836	926.3	892.0	3.08	3.09	1,072	.3047
3	27	1	F <sub>1</sub>	G	.920	.994	.0022	66.22	8.14	2,444	.4236	1,035.4	817	.789	967.7	974.1	3.22	3.24	1,030	.2984
3	27	2	E <sub>1</sub>	G	1.055	1.097	.0021	69.37	8.33	2,444	---	---	---	---	1,085.3	989.1	3.61	3.29	1,237	.3270
3	27	3	D <sub>1</sub>	G	1.212	1.450	.0035	41.62	6.45	2,444	.4665	1,140.2	---	---	1,199.2	826.8	3.99	2.75	2,517	.4667
3	27	4	F <sub>1</sub>	G	1.219	1.508	.0039	37.35	6.11	2,444	.4755	1,162.2	1,345	1.157	1,201.6	796.7	4.00	2.65	2,815	.4936
3	29	1	F <sub>1</sub>	G	.846	.960	.0024	60.70	7.79	2,444	.4324	1,056.9	886	.838	906.2	944.0	3.01	3.14	985	.2920
3	30	1	F <sub>1</sub>	G	.877	.992	.0024	60.70	7.79	2,444	.4324	1,056.9	898	.850	936.4	944.0	3.11	3.14	1,052	.3017

\*A run is defined as one operation of the blowdown tunnel from valve opening to valve closing.

†Chronological order in which recorded points occurred during the test run.

TABLE II.-- COMPILATION OF ANALYTICAL AND TEST RESULTS - Continued

(e) 452 Platform

Model	Run*	Point†	Wing panel behavior		Me	Ve/VR	Pe' slugs cu ft	We	Ve	ω <sub>R</sub> radians/sec	ω <sub>R</sub> /ω <sub>b</sub>	α <sub>R</sub> ' radians/sec	α <sub>e</sub> ' radians/sec	ω <sub>e</sub> /ω <sub>R</sub>	Ve' ft/sec	VR' ft/sec	Ve/b <sub>0</sub> ω <sub>b</sub>	VR/b <sub>0</sub> ω <sub>b</sub>	q <sub>e</sub> ' lb/sq ft	Ve/b <sub>0</sub> ω <sub>b</sub>  Ve
			Left	Right																
1	1	1	N	F <sub>1</sub>	0.817	0.916	0.0032	51.59	7.18	2,300	0.4748	1,092	1,005	0.920	847.7	925.3	3.44	3.76	1,150	0.3149
1	1	2	D <sub>1</sub>	F <sub>1</sub>	.824	.938	.0035	47.59	6.90	2,300	.4830	1,111	-----	-----	845	901	3.43	3.66	1,250	.3266
1	1	3	F <sub>1</sub>	F <sub>1</sub>	.821	.951	.0037	44.26	6.66	2,300	.4900	1,127	999	.886	835	878	3.39	3.57	1,290	.3344
1	1	1	F <sub>1</sub>	F <sub>1</sub>	.900	.963	.0029	57.36	7.57	2,300	.4638	1,067	906	.849	924.7	959.8	3.76	3.90	1,240	.3258
1	1	1	D <sub>1</sub>	G	.932	.967	.0027	60.26	7.76	2,300	.4582	1,054	-----	-----	945.2	977	3.84	3.97	1,206	.3249
1	1	2	F <sub>1</sub>	G	1.001	1.038	.0028	59.24	7.70	2,300	.4600	1,058	964	.911	1,006.5	969.6	4.09	3.94	1,418	.3487
1	1	1	F <sub>1</sub>	G	1.118	1.023	.0021	77.31	8.79	2,300	-----	-----	-----	-----	1,089.7	1,065.6	4.43	4.33	1,247	.3307
1	1	1	E <sub>1</sub>	G	1.290	1.126	.0020	81.12	9.01	2,300	-----	-----	-----	-----	1,222.5	1,085.3	4.97	4.41	1,494	.3619
1	1	3	D <sub>2</sub>	G	1.386	1.275	.0027	61.67	7.86	2,300	.4554	1,047	-----	-----	1,255	984	5.10	4.00	2,126	.4259
1	1	4	F <sub>2</sub>	G	1.412	1.297	.0027	60.99	7.82	2,300	.4565	1,050	-----	-----	1,271	980	5.16	3.98	2,181	.4335
1	1	1	F <sub>1</sub>	G	1.123	1.042	.0022	75.51	8.69	2,300	.4313	992	1,005	1.013	1,102.7	1,058.2	4.48	4.30	1,358	.3385
1	1	2	E <sub>1</sub>	G	1.200	1.082	.0021	78.83	8.88	2,300	-----	-----	-----	-----	1,163.4	1,075.5	4.73	4.37	1,421	.3495
1	1	3	D <sub>2</sub>	G	1.356	1.270	.0027	60.68	7.79	2,300	.4573	1,052	-----	-----	1,244.3	979.5	5.06	3.98	2,090	.4261
1	1	4	F <sub>2</sub>	G	1.419	1.316	.0027	60.21	7.76	2,300	.4582	1,054	1,120	1.063	1,285.6	977	5.22	3.97	2,231	.4419
1	1	1	D <sub>1</sub>	G	1.006	.993	.0024	67.24	8.20	2,300	.4455	1,025	-----	-----	1,009.5	1,016.4	4.10	4.13	1,223	.3284
1	1	2	F <sub>1</sub>	G	1.066	1.038	.0025	67.19	8.20	2,300	.4455	1,025	916	.894	1,055.4	1,016.4	4.29	4.13	1,392	.3433
1	1	1	D <sub>1</sub>	G	.991	.980	.0024	67.77	8.23	2,300	.4445	1,022	-----	-----	998.1	1,018.9	4.06	4.14	1,195	.3235
1	1	2	F <sub>1</sub>	G	1.103	1.062	.0024	69.16	8.32	2,300	.4420	1,017	942	.926	1,089.9	1,026.2	4.43	4.17	1,425	.3494
1	1	1	F <sub>1</sub>	N	1.285	1.123	.0022	75.27	8.68	2,300	.4315	992	-----	-----	1,185.2	1,055.8	4.82	4.29	1,545	.3642
1	1	1	F <sub>1</sub>	N	1.189	1.082	.0024	68.96	8.30	2,300	.4425	1,018	1,062	1.043	1,107.3	1,023.8	4.50	4.16	1,471	.3558
1	1	2	F <sub>1</sub>	F <sub>1</sub>	1.223	1.122	.0025	65.30	8.08	2,300	.4490	1,033	1,100	1.065	1,127	1,004.1	4.58	4.08	1,588	.3720
1	1	1	F <sub>1</sub>	F <sub>1</sub>	1.006	1.016	.0029	56.24	7.50	2,300	.4657	1,071	1,068	.997	967.7	952.4	3.93	3.87	1,358	.3442
1	1	1	F <sub>1</sub>	F <sub>1</sub>	1.023	1.030	.0030	55.32	7.44	2,300	.4674	1,075	1,062	.988	975.7	947.5	3.96	3.85	1,428	.3498
1	1	1	F <sub>1</sub>	F <sub>1</sub>	1.097	1.041	.0026	64.15	8.01	2,300	.4510	1,037	1,049	1.012	1,037.5	996.7	4.22	4.05	1,399	.3455
1	1	1	F <sub>1</sub>	F <sub>1</sub>	.660	.894	.0066	24.95	5.00	2,300	-----	-----	-----	-----	653	730.9	2.65	2.97	1,407	.3484
1	1	2	G	F <sub>1</sub>	.797	.941	.0042	39.43	6.28	2,300	.5008	1,152	1,037	.900	794.1	844.1	3.23	3.43	1,324	.3373

\*A run is defined as one operation of the blowdown tunnel from valve opening to valve closing.

†Chronological order in which recorded points occurred during the test run.

TABLE II.- COMPILATION OF ANALYTICAL AND TEST RESULTS - Continued

(f) 460 Planform

Model	Run*	Point†	Wing panel behavior		M <sub>e</sub>	V <sub>e</sub> /V <sub>R</sub>	ρ <sub>e</sub> , slugs/cu ft	H <sub>e</sub>	√H <sub>e</sub>	ω <sub>R</sub> , radians/sec	ω <sub>R</sub> /ω <sub>a</sub>	ω <sub>R</sub> , radians/sec	ω <sub>e</sub> , radians/sec	ω <sub>e</sub> /ω <sub>R</sub>	V <sub>e</sub> , ft/sec	V <sub>R</sub> , ft/sec	V <sub>e</sub> /V <sub>R</sub>	q <sub>e</sub> , lb/sq ft	V <sub>e</sub> /b <sub>0</sub> ω <sub>e</sub> √H <sub>e</sub>
			Left	Right															
1	1	1	F1	N	1.316	1.114	0.0020	---	---	---	---	---	---	---	1,097	---	---	---	---
1	1	2	F1	F1	1.304	1.121	0.0020	120.19	10.96	0.3104	---	804.2	---	1.149	1,213.4	1,082.1	6.26	1,472	0.3012
1	1	1	F1	N	1.003	1.001	0.0029	86.16	9.28	.3378	2,255	791.7	1.030	1.030	985.7	984.6	5.04	1,409	.2863
1	1	1	F1	N	.986	.986	0.0028	86.37	9.29	.3377	2,276	768.6	1.014	1.014	970.6	984.6	4.96	1,319	.2816
1	1	2	F1	D1	1.019	1.025	0.0029	85.20	9.25	.3387	2,255	763.8	---	---	971.6	971.6	5.14	1,439	.2936
1	1	3	F1	F1	1.032	1.037	0.0029	84.61	9.20	.3393	2,255	765.1	1.002	1.002	969.7	969.7	5.00	1,465	.2973
1	1	1	F1	D1	.959	.981	0.0030	82.40	9.08	.3412	2,255	769.4	.988	.988	945.6	963.8	4.88	1,341	.2833
1	1	2	F1	F1	.989	1.009	0.0030	81.42	9.02	.3422	2,255	771.7	.985	.985	968.9	960	5.00	1,408	.2922
1	1	1	F1	N	.960	.972	0.0030	82.26	9.07	.3414	2,276	777	1.022	1.022	945.1	972.8	4.83	1,340	.2809
1	1	2	F1	F1	.960	.982	0.0030	82.51	9.08	.3412	2,255	769.4	.931	.931	963.8	963.8	4.88	1,344	.2836
1	1	1	F1	F1	.918	.951	0.0030	81.99	9.05	.3418	2,255	770.8	.880	.880	914.7	961.9	4.72	1,255	.2750
2	2	1	N	F1	1.039	1.047	0.0032	75.83	8.71	.3344	2,399	802.2	1.061	1.061	995.6	951.1	4.83	1,586	.2923
2	2	2	F1	F1	1.076	1.043	0.0032	76.73	8.76	.3240	2,522	817.1	1.069	1.069	1,022.7	980.3	4.72	1,673	.2840
2	2	1	F1	F1	.985	.970	0.0032	78.78	8.88	.3222	2,522	812.6	1.075	1.075	961.7	991.2	4.43	1,434	.2634
2	2	1	N	F1	1.068	1.039	0.0030	80.83	8.99	.3300	2,399	791.7	1.040	1.040	1,008	969.7	4.85	1,524	.2857
2	2	2	F1	F1	1.062	1.012	0.0031	78.95	8.89	.3200	2,522	812.1	1.075	1.075	1,003.3	991.2	4.63	1,560	.2745
2	2	1	F1	F1	1.286	1.050	0.0021	115.17	10.73	.2945	2,522	742.7	1.117	1.117	1,179.3	1,123.5	5.14	1,460	.2674
2	2	1	N	F1	1.120	1.034	0.0027	89.88	9.48	.3223	2,399	823.1	1.065	1.065	1,039.8	1,005.8	5.04	1,460	.2805
2	2	2	D1	F1	1.127	1.021	0.0028	86.80	9.32	.3155	2,522	795.7	---	---	1,043.5	1,021.6	4.81	1,524	.2724
2	2	3	F1	F1	1.127	1.023	0.0028	87.04	9.33	.3153	2,522	867.1	1.090	1.090	1,045	1,021.6	4.82	1,529	.2724
2	2	1	N	F1	1.103	1.061	0.0030	80.83	8.99	.3300	2,399	829.4	1.048	1.048	969.7	969.7	4.99	1,587	.2926
2	2	2	D1	F1	1.103	1.031	0.0030	80.83	8.99	.3206	2,522	808.6	---	---	997.7	997.7	4.74	1,587	.2783
2	2	3	F1	F1	1.103	1.031	0.0030	80.83	8.99	.3206	2,522	808.6	1.080	1.080	997.7	997.7	4.74	1,587	.2974
2	2	1	F1	N	1.178	1.003	0.0025	99.66	9.98	.2967	2,645	860.8	1.097	1.097	1,096.4	1,096.4	4.83	1,511	.2555
2	2	1	F1	F1	.821	.902	0.0050	49.28	7.02	.3500	2,522	882.7	.982	.982	772.6	856.7	3.56	1,492	.2677
2	2	1	D1	G	1.356	1.039	0.0020	124.64	11.16	---	2,645	---	---	---	1,180.6	1,180.6	5.39	1,504	.2549
2	2	1	F1	G	1.374	1.049	0.0020	123.77	11.13	.2800	2,645	740.6	1.179	1.179	1,238.4	1,180.6	5.14	1,534	.2581
2	2	1	D1	G	1.262	1.004	0.0021	117.71	10.85	.2840	2,645	731.2	---	---	1,164.7	1,160.1	5.12	1,424	.2490
2	2	2	F1	G	1.294	1.037	0.0022	113.16	10.64	.2871	2,645	759.4	1.150	1.150	1,184.8	1,143	5.21	1,544	.2583
3	3	1	D1	G	.924	.989	0.0034	72.12	8.49	.3485	2,399	836	.947	.947	969.7	969.7	4.65	1,562	.2888
3	3	2	F1	G	.888	.981	0.0037	66.27	8.14	.3561	2,399	898.5	1.052	1.052	923	940.8	4.47	1,576	.2900
4	4	1	N	F1	.837	.873	0.0043	57.03	7.55	.3689	2,676	889.1	.901	.901	870.3	996.5	3.78	1,628	.2643
4	4	1	X	D1	.928	.953	0.0044	55.73	7.46	.3703	2,676	930.9	---	---	943.1	989.6	4.10	1,957	.2898
4	4	2	X	F1	.937	.994	0.0049	50.04	7.07	.3791	2,676	1,014.5	.912	.912	947.2	952.8	4.12	1,98	.3071
5	5	1	F1	F1	.867	1.060	0.0046	67.90	8.24	.2750	2,821	775.8	1.114	1.114	905.4	854	3.73	1,885	.2390

\* A run is defined as one operation of the blowdown tunnel from valve opening to valve closing.

† Chronological order in which recorded points occurred during the test run.

TABLE II.- COMPILATION OF ANALYTICAL AND TEST RESULTS - Concluded

(g) 645 Planform

Model	Run*	Point†	Wing panel behavior		M <sub>e</sub>	V <sub>e</sub> /V <sub>R</sub>	P <sub>e</sub> * slugs cu ft	h <sub>e</sub>	h <sub>c</sub>	ω <sub>w</sub> radians sec	ω <sub>R</sub> /ω <sub>w</sub>	ω <sub>w</sub> radians sec	ω <sub>e</sub> radians sec	ω <sub>e</sub> /ω <sub>R</sub>	V <sub>e</sub> ft/sec	V <sub>R</sub> ft/sec	V <sub>e</sub> b <sub>tab</sub>	V <sub>R</sub> b <sub>tab</sub>	q <sub>e</sub> lb/sq ft	V <sub>e</sub> b <sub>tab</sub> /√h <sub>e</sub>
			Left	Right																
1	1	1	D1	G	1.361	1.271	0.0028	62.41	7.90	3.179	0.3538	1.125	---	---	977.2	4.15	3.27	2,161	0.3895	
1	2	2	F1	G	1.321	1.351	0.0035	50.45	7.10	3.179	.3659	1,163	1,313	1.129	1,215.5	899.5	4.06	3.01	2,586	0.4240
1	1	1	D1	G	.964	.899	0.0024	73.69	8.59	3.179	.3436	1,092	---	---	1,066.8	3.14	3.50	1,060	.2710	
1	2	2	F1	G	1.081	1.081	0.0023	76.90	8.78	3.179	.3405	1,082	---	---	1,066.8	3.45	3.57	1,228	.2915	
1	3	3	E1	G	1.235	1.070	0.0023	78.19	8.84	3.179	.3598	1,080	---	---	1,069.8	3.82	3.58	1,507	.3207	
1	4	4	D2	G	1.316	1.250	0.0029	59.98	7.74	3.179	.3562	1,132	---	---	962.2	4.02	3.22	2,097	.3848	
1	5	5	F2	G	1.311	1.320	0.0034	51.63	7.19	3.179	.3616	1,159	---	---	908.4	4.00	3.04	2,444	0.4130	
1	3	1	F1	G	1.055	.985	0.0024	72.52	8.52	3.179	.3445	1,095	.942	.860	1,021.7	3.41	3.47	1,253	.2970	
1	4	1	F1	G	1.153	.938	0.0018	98.25	9.92	3.179	---	---	1,401	---	1,106.9	3.70	3.95	1,103	.2764	
1	1	2	E1	G	1.270	.964	0.0016	110.53	10.51	3.179	---	---	---	---	1,195.1	3.99	4.15	1,143	.2816	
1	1	3	D2	G	1.356	1.285	0.0030	58.86	7.67	3.179	.3573	1,136	---	---	1,288.5	4.10	3.20	2,264	.3967	
1	1	4	F2	G	1.354	1.272	0.0035	51.19	7.65	3.179	.3576	1,137	1,376	1.210	1,216.7	956	4.06	3.19	2,591	.3999
1	5	1	D1	N	1.315	1.333	0.0035	50.30	7.09	3.179	.3661	1,164	---	---	1,199.1	4.00	3.01	2,516	0.4189	
1	1	2	F1	N	1.316	1.367	0.0038	46.70	6.83	3.179	.3701	1,176	1,382	1.175	1,193	872.6	3.98	2.92	2,704	0.3225
1	6	1	D1	N	1.320	1.301	0.0033	53.13	7.29	3.179	.3631	1,154	---	---	1,197.6	4.00	3.08	2,366	0.4069	
1	1	2	F1	N	1.308	1.308	0.0035	51.24	7.16	3.179	.3650	1,160	1,414	1.219	1,184	905.4	3.95	3.03	2,453	0.4096
1	1	1	F1	F1	1.041	.974	0.0025	70.33	8.39	3.179	.3466	1,102	942	.855	1,001.3	1,028	3.34	3.44	1,253	.2956
1	8	1	F1	F1	1.095	.987	0.0024	74.79	8.65	3.179	.3426	1,089	1,005	.923	1,037.8	1,051.9	3.47	3.52	1,292	.2972
1	1	2	E1	D1	1.205	1.086	0.0023	76.40	8.74	3.179	.3412	1,085	---	---	1,152.2	1,060.8	3.85	3.55	1,527	.3265
1	3	3	D2	D2	1.279	1.202	0.0027	66.09	8.13	3.179	.3504	1,114	---	---	1,202.9	1,001.1	4.02	3.35	1,953	.3665
1	1	4	F2	F2	1.277	1.248	0.0030	58.94	7.68	3.179	.3572	1,136	1,238	1.090	1,193.2	956.2	3.98	3.20	2,136	.3848
1	1	1	F1	F1	1.034	.983	0.0026	68.90	8.30	3.179	.3578	1,137	961	.845	1,001.3	1,019	3.34	3.41	1,305	.2988
1	10	1	F1	F1	1.078	.982	0.0023	77.44	8.80	3.179	.3402	1,081	1,074	.994	1,047.5	1,066.8	3.50	3.57	1,262	.2948
1	1	2	E1	E1	1.220	1.068	0.0022	79.46	8.91	3.179	---	---	---	---	1,152.5	1,078.8	3.85	3.61	1,461	.3204
1	1	1	F1	F1	1.103	.974	0.0022	79.74	8.93	3.179	---	---	1,382	---	1,094.2	1,081.8	3.52	3.62	1,222	.2924
1	1	1	F1	F1	.981	.985	0.0028	62.85	7.93	3.179	.3534	1,123	1,049	.934	955.7	980.1	3.19	3.28	1,279	.2985
1	1	1	F1	F1	.877	.941	0.0033	54.14	7.36	3.179	.3620	1,151	967	.840	868.6	923.4	2.90	3.09	1,245	.2925
1	1	1	F1	F1	.832	.935	0.0037	48.39	6.96	3.179	.3681	1,170	1,023	.874	827.3	884.5	2.76	2.96	1,266	.2944
1	1	1	D1	D1	.775	.917	0.0042	42.11	6.50	3.179	.3751	1,192	---	---	769.9	839.7	2.57	2.81	1,243	.2934
1	1	2	F1	F1	.763	.917	0.0043	41.13	6.42	3.179	.3763	1,196	1,047	.875	761.5	830.7	2.54	2.78	1,247	.2938
1	1	1	D1	D1	.848	.925	0.0034	52.47	7.24	3.179	.3638	1,156	---	---	845.9	914.4	2.82	3.06	1,216	.2894
1	1	2	F1	F1	.891	.981	0.0035	50.30	7.09	3.179	.3661	1,164	1,062	.912	982.1	899.5	2.95	3.01	1,362	.3431
1	1	1	F1	F1	1.040	.979	0.0026	69.33	8.33	3.179	.3474	1,104	1,018	.922	1,003.3	1,025	3.35	3.43	1,308	.2983
1	1	1	F1	X	1.014	1.005	0.0030	59.55	7.72	3.179	.3566	1,134	1,049	.925	967.4	962.2	3.23	3.22	1,404	.3104

\* A run is defined as one operation of the blowdown tunnel from valve opening to valve closing.

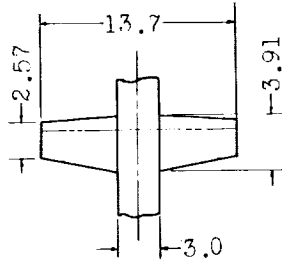
† Chronological order in which recorded points occurred during the test run.

A = 2.4

A = 4

A = 6.4

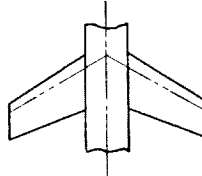
$\Lambda = 0^\circ$



400

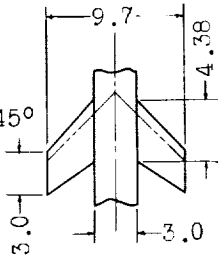
Planform designation

$\Lambda = 30^\circ$

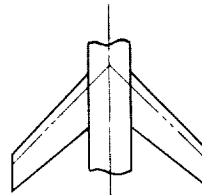


430

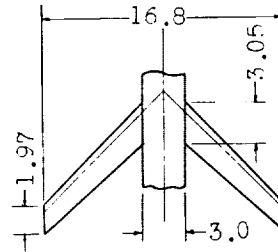
$\Lambda = 45^\circ$



245

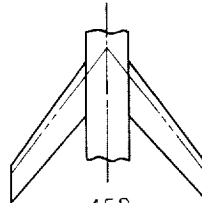


445



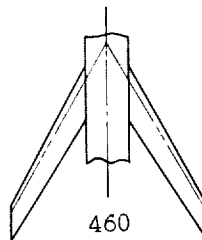
645

$\Lambda = 52\frac{1}{2}^\circ$



452

$\Lambda = 60^\circ$



460

Note: Dimensions shown (inches) are constant for a given aspect ratio.

Figure 1.- Planform sketches of flutter models giving aspect ratio, sweep angle, planform dimensions, and model designations.

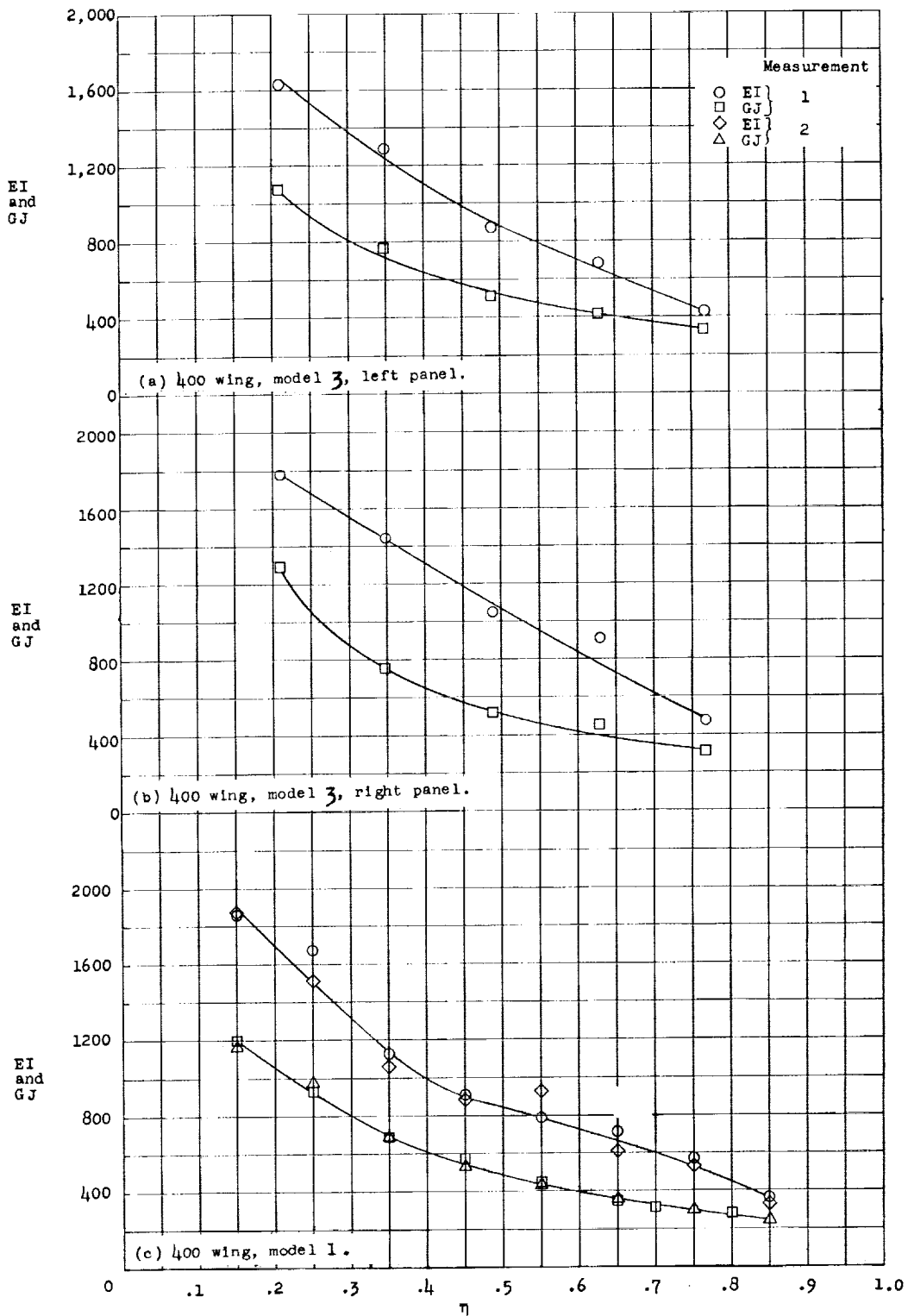


Figure 2.- Measured variation of bending and torsional stiffness along the span for 400 wings.

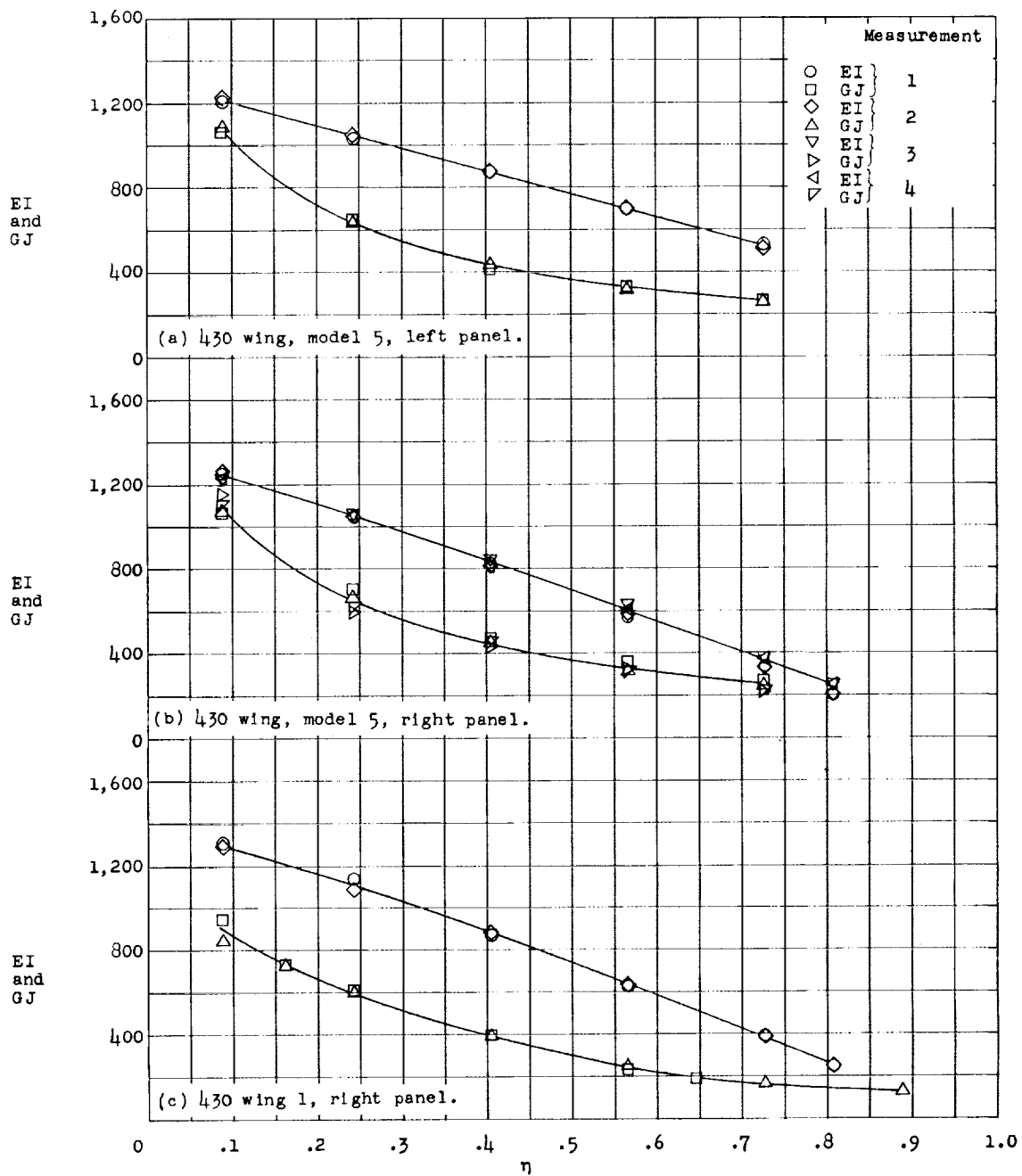


Figure 3.- Measured variation of bending and torsional stiffness along the span for 430 wings.

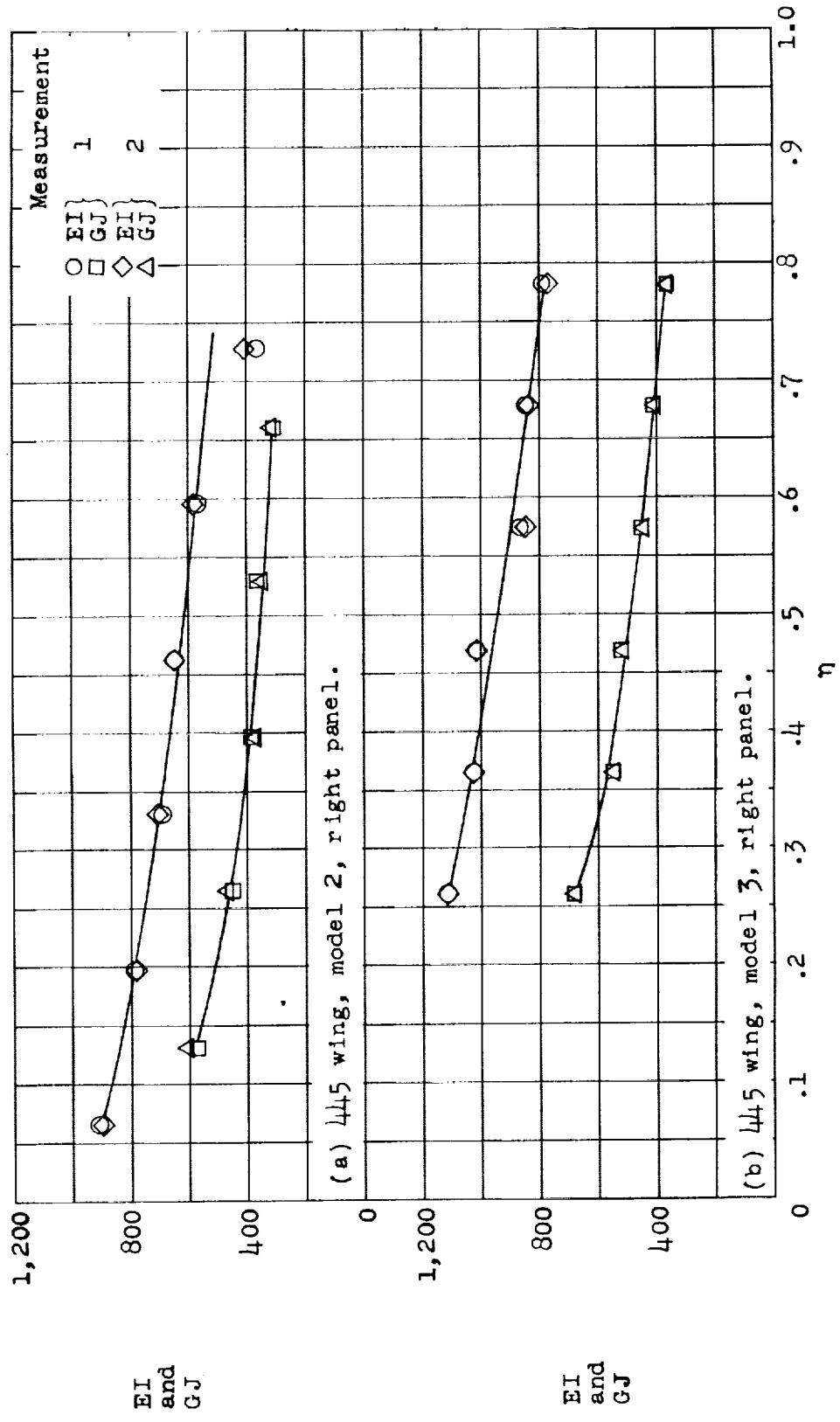


Figure 4.- Measured variation of bending and torsional stiffness along the span for 445 wings.

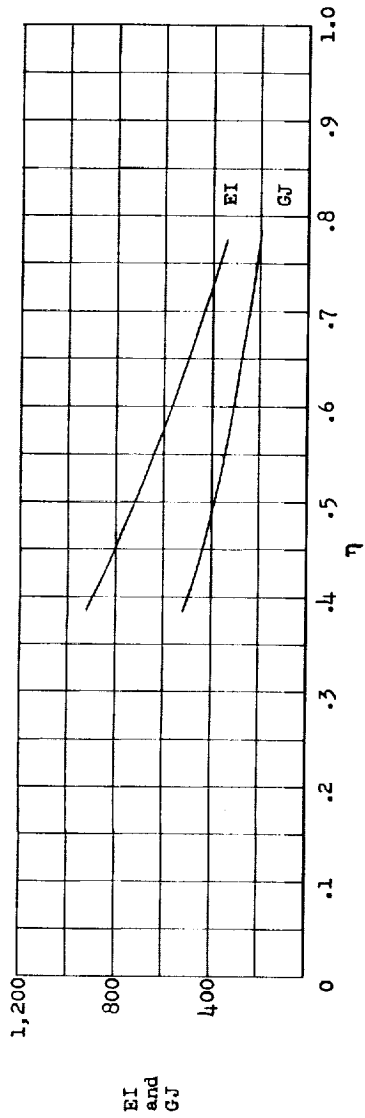


Figure 5.- Measured variation of bending and torsional stiffness along the span for 452 wing, model 1.

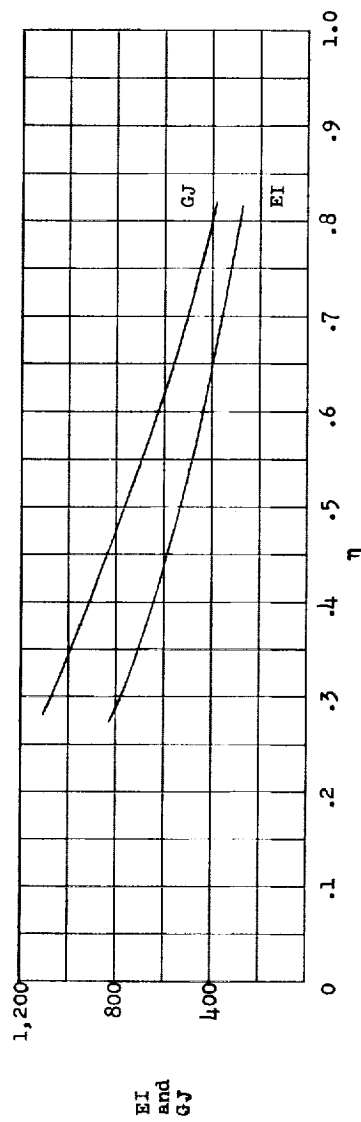


Figure 6.- Spanwise variations of the estimated bending and torsional stiffness of the 645 magnesium wing. Values were scaled from the measured variation on a similar wing of 2017-Γ aluminum alloy as follows:  $(EI)_{Mg} = (EI)_{Al} \times \frac{E_{Mg}}{E_{Al}}$

$$\text{and } (GJ)_{Mg} = (GJ)_{Al} \times \frac{G_{Mg}}{G_{Al}}.$$

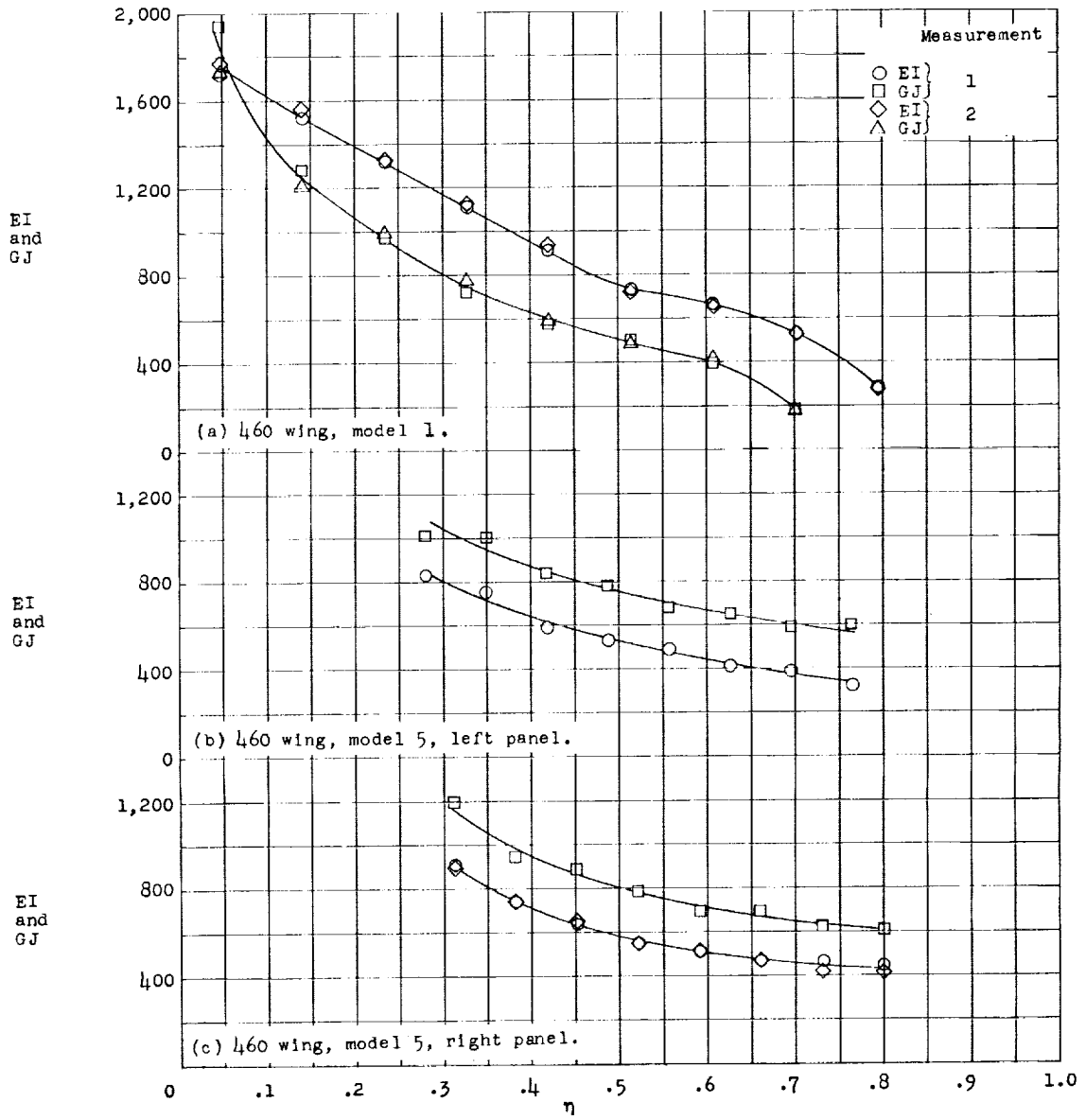


Figure 7.- Measured variation of bending and torsional stiffness along the span for 460 wings.

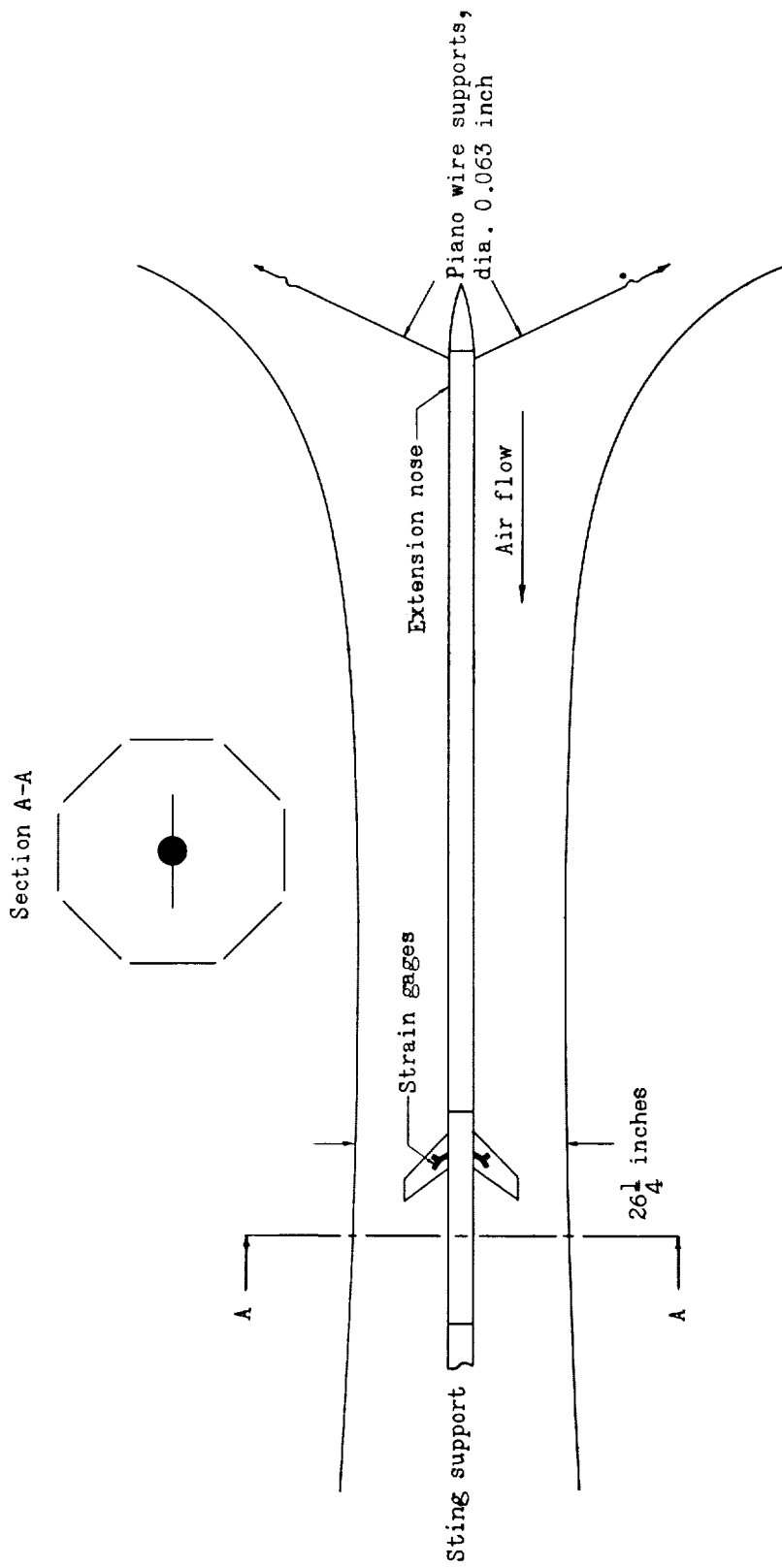


Figure 8.- Plan view of Langley transonic blowdown tunnel with flutter model installed.

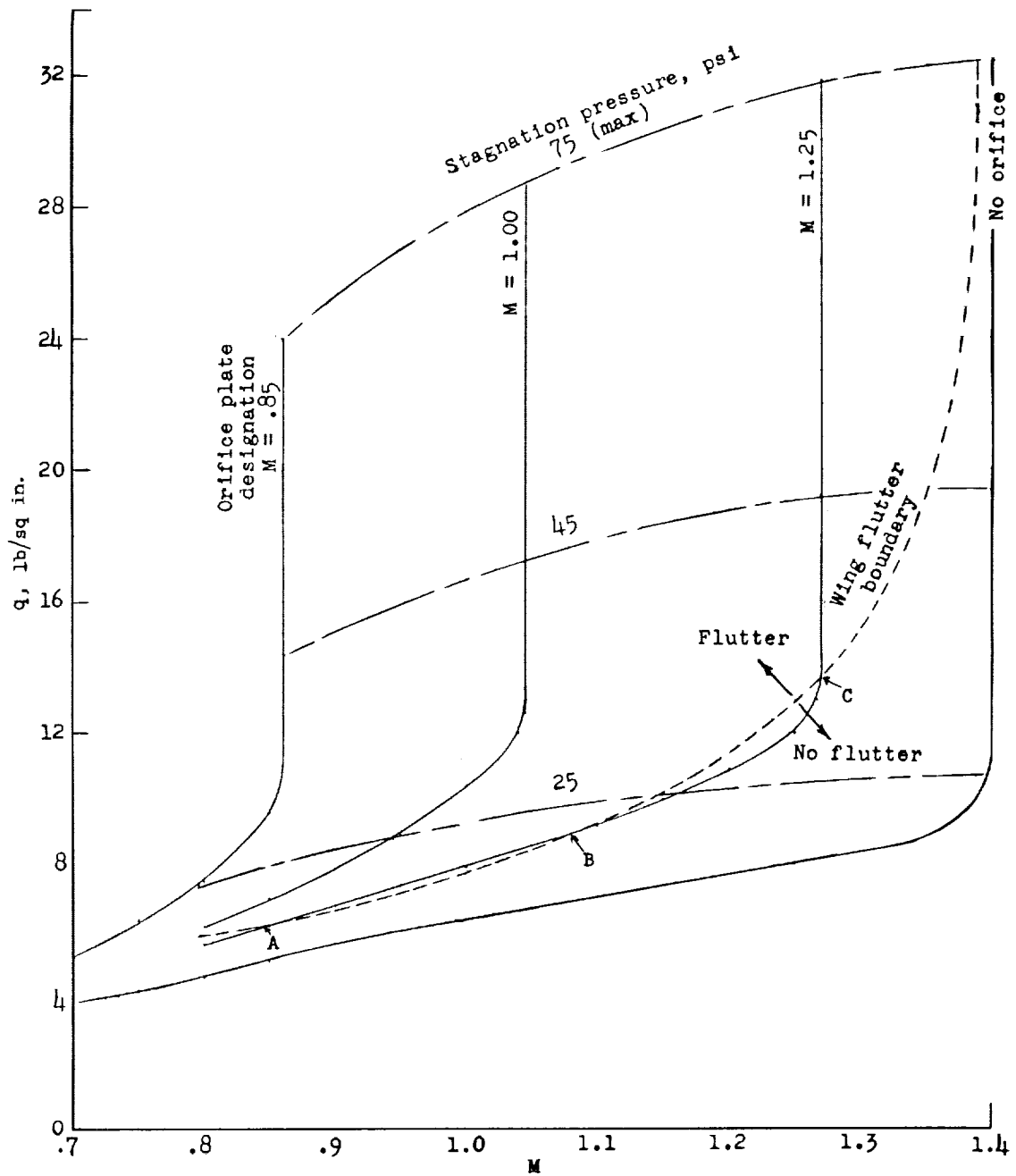
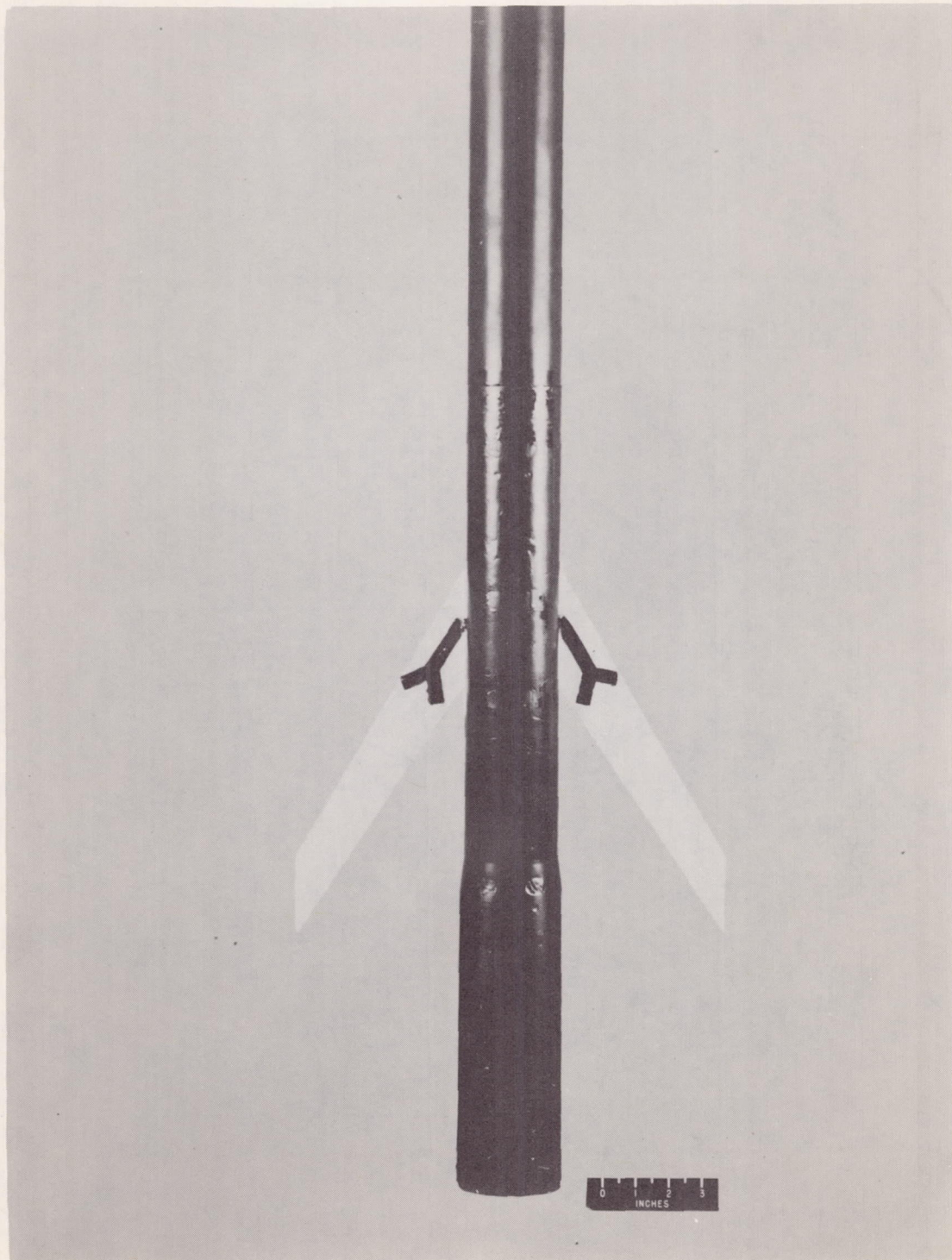


Figure 9.- Variation with Mach number of tunnel dynamic-pressure curves for several orifice conditions, and an example wing-flutter-boundary curve.



L-79715.1

Figure 10.- Example of flutter model mounted on sting fuselage.

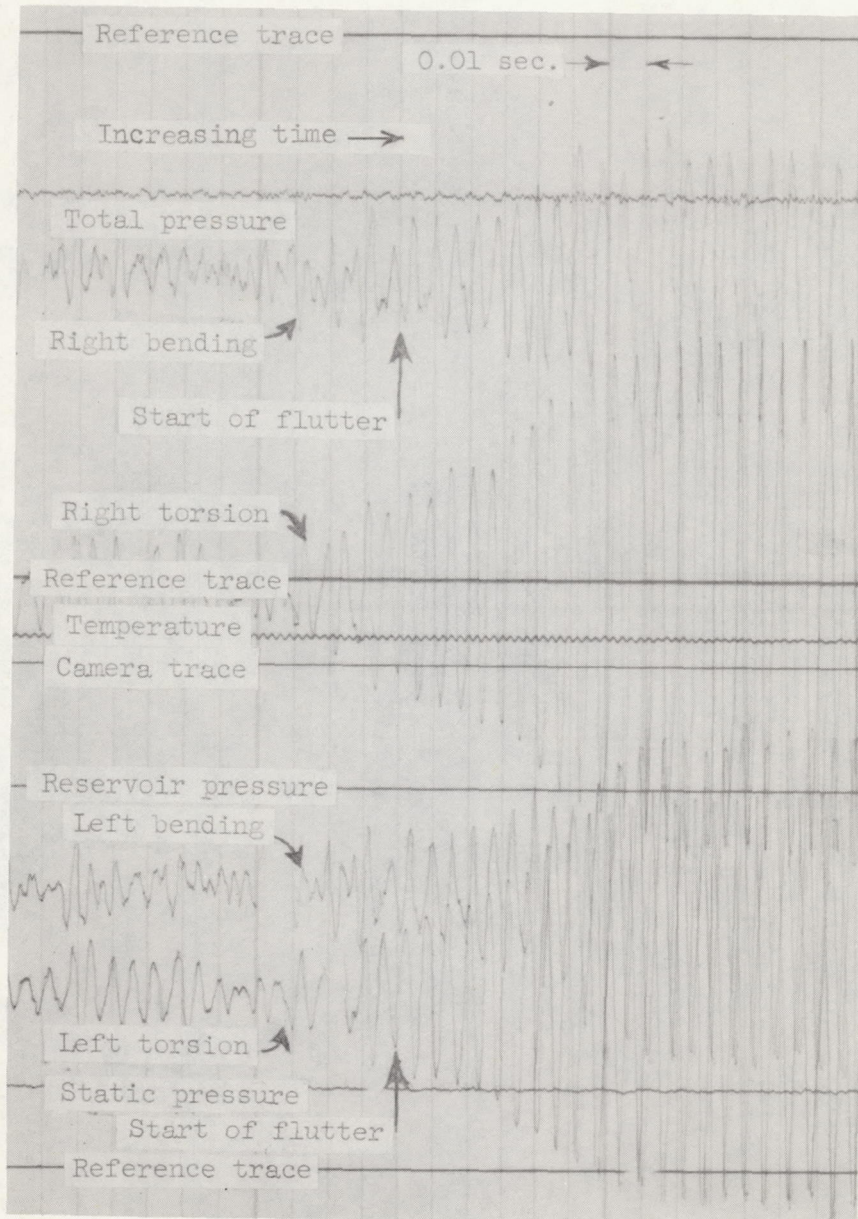


Figure 11.- Sample oscillograph record of flutter test (445 wing at  $M = 0.813$ ).

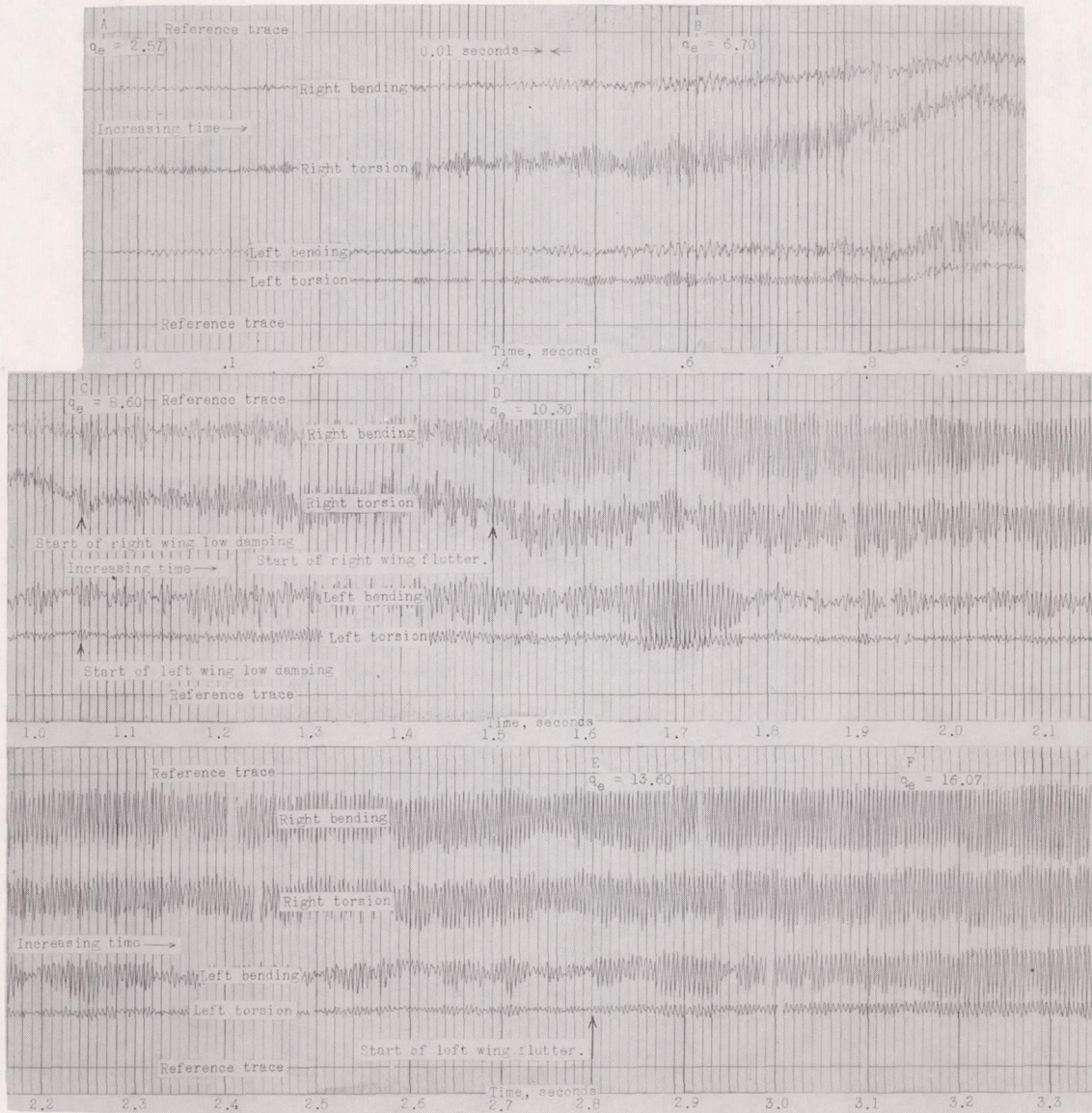
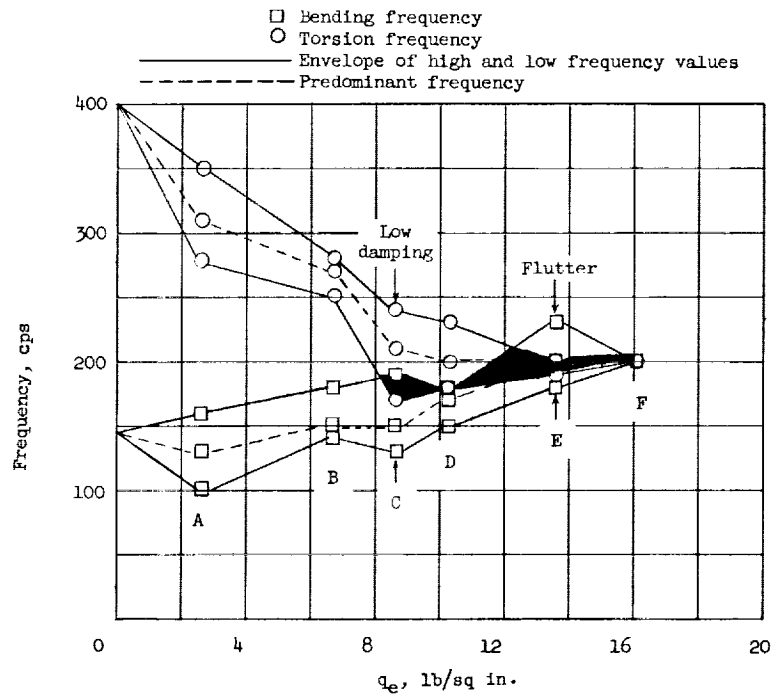
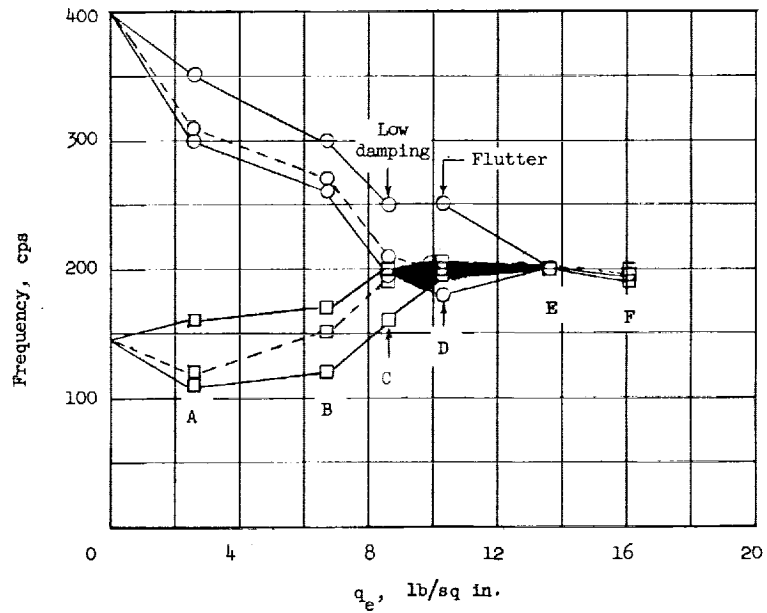


Figure 12.- Tracing of a section of an oscillograph record showing low damping and flutter which occurred on a 400 wing during a flutter test run.

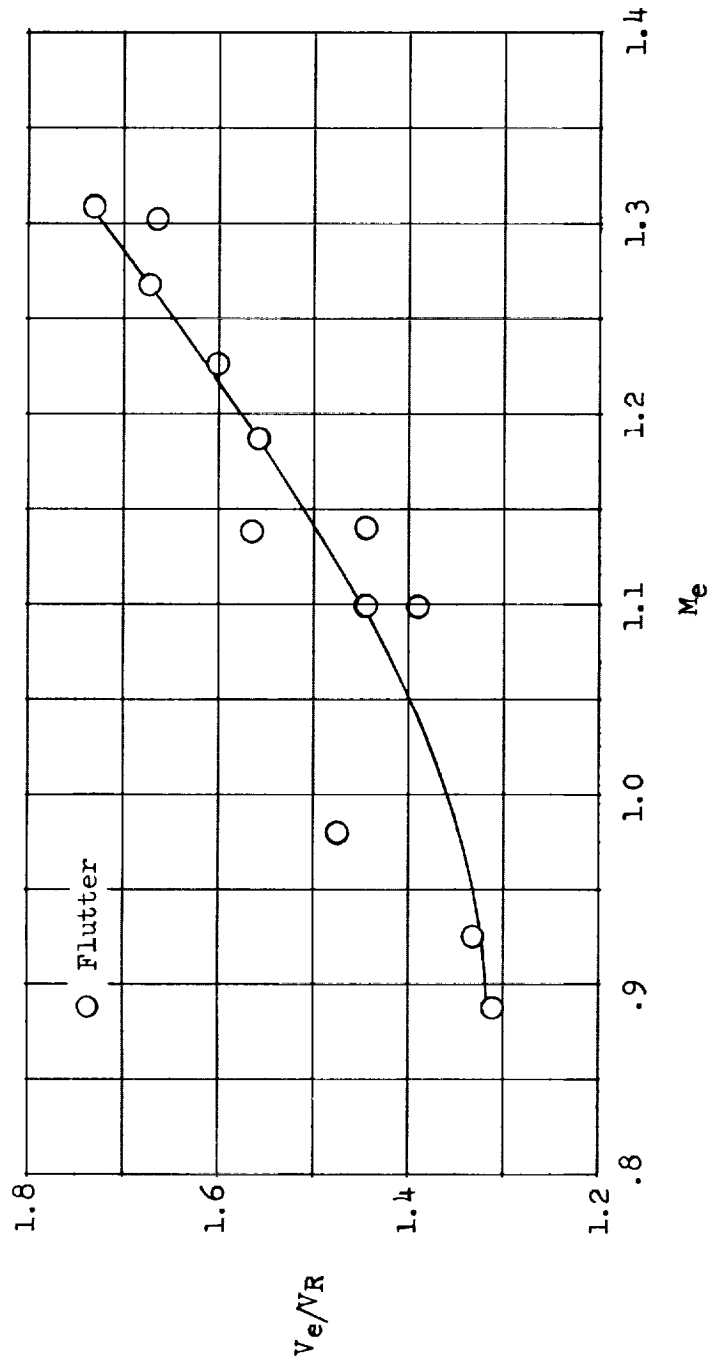


(a) Left wing panel.



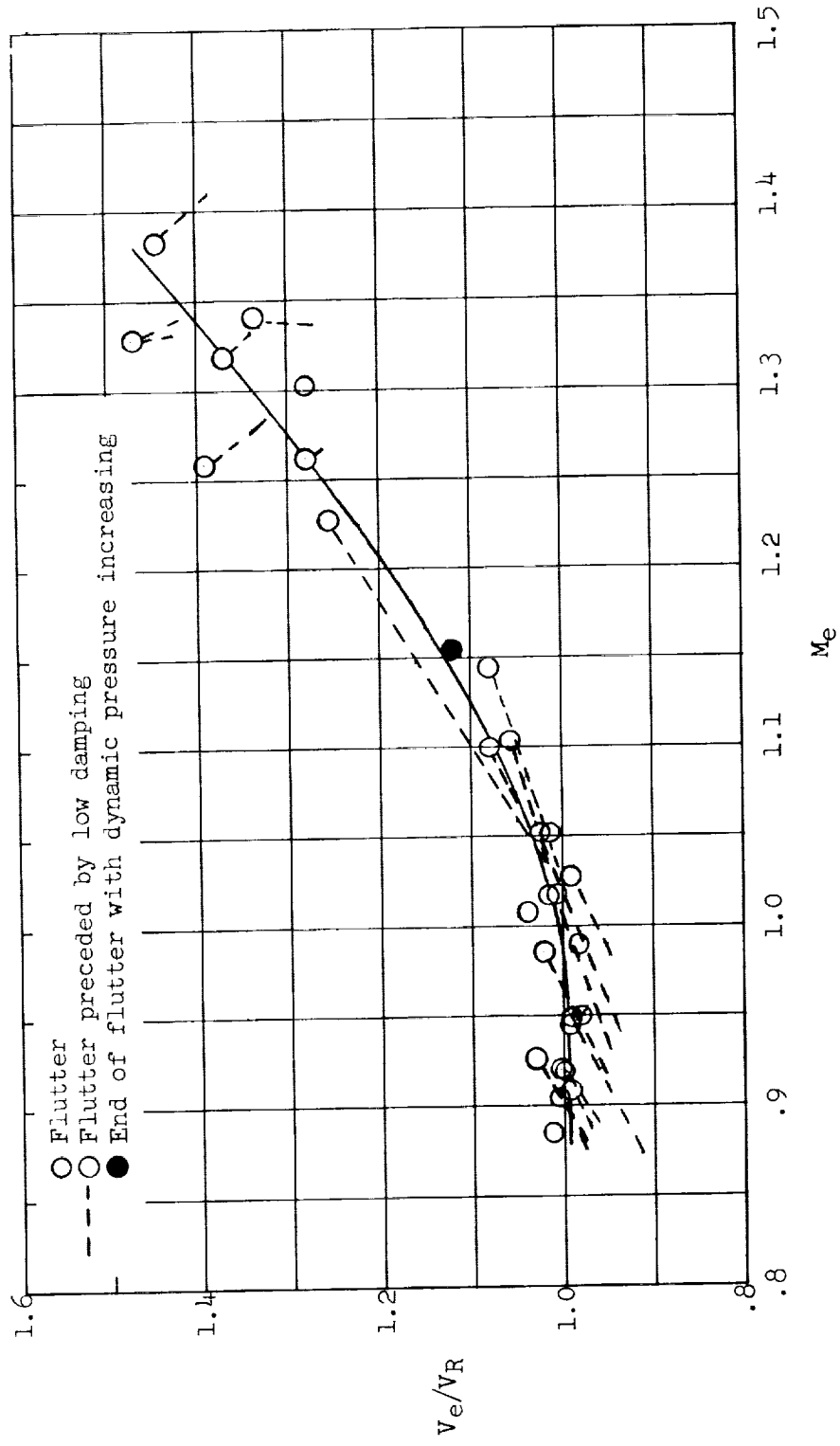
(b) Right wing panel.

Figure 13.- Variation of bending and torsion frequencies of a 400 wing with dynamic pressure during a test run. Shaded areas indicate low damping region.



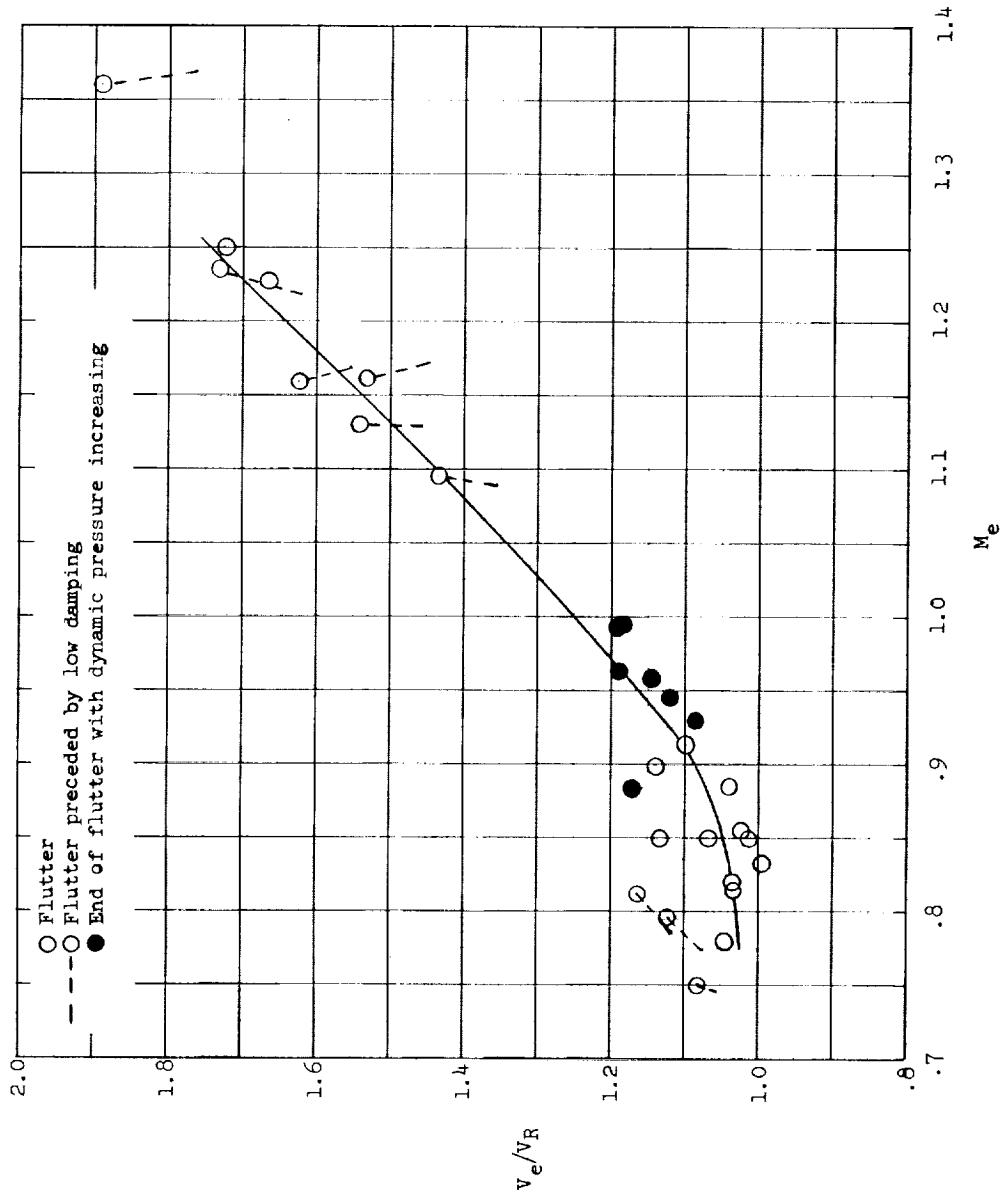
(a) 245 planform.

Figure 14.- Variation of flutter-speed ratio with Mach number for the various flutter-model planforms.



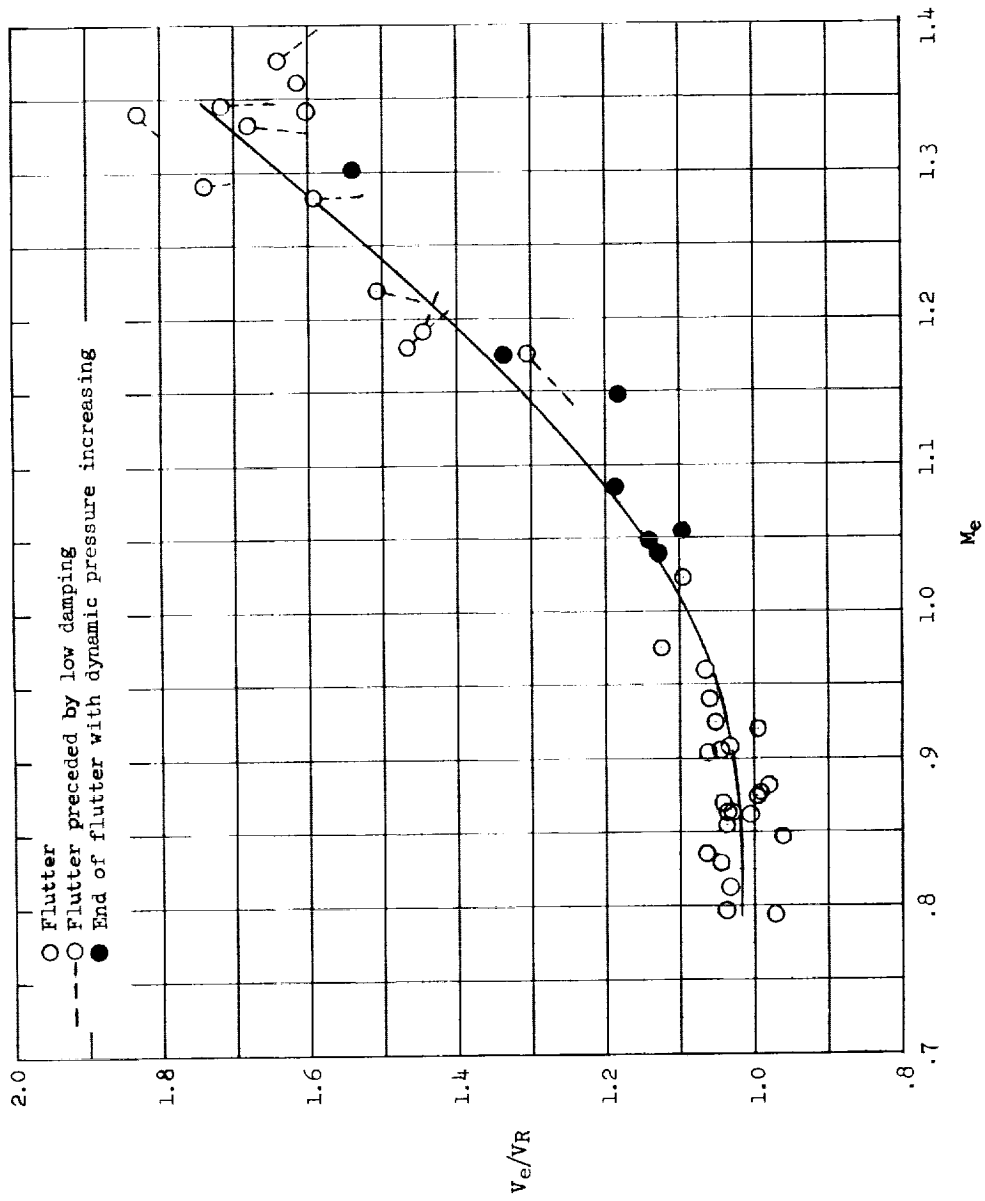
(b) 400 planform.

Figure 14.- Continued.

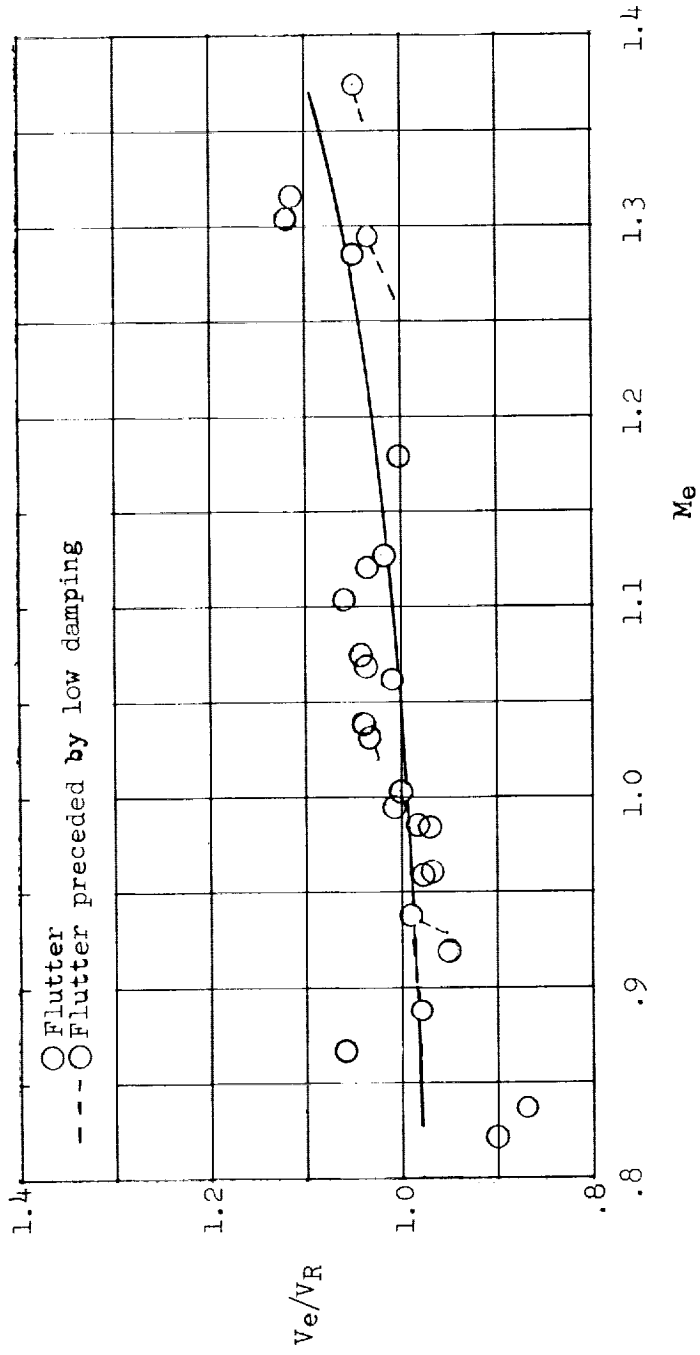


(c) 430 planform.

Figure 14.- Continued.

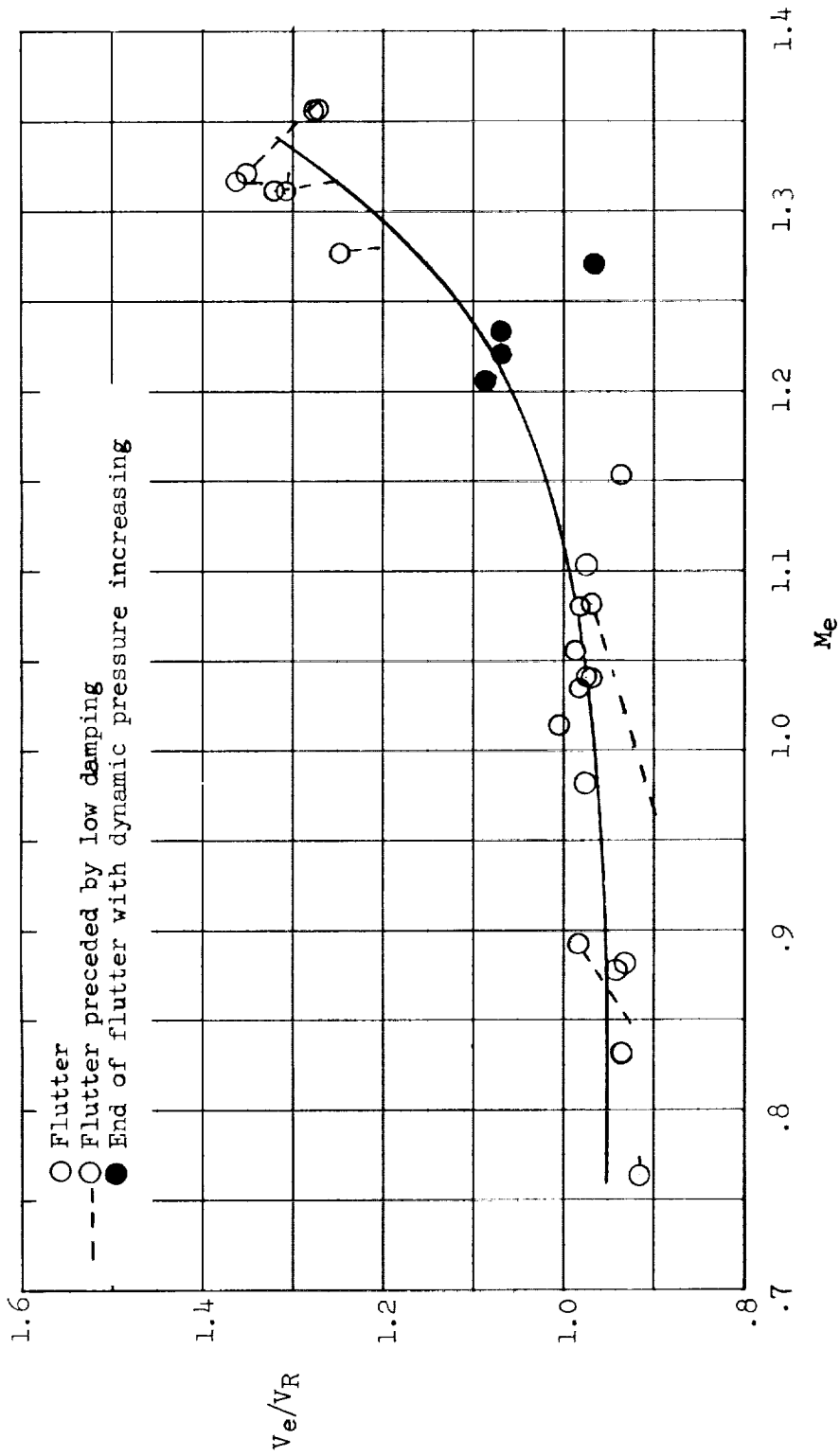






(f) 460 planform.

Figure 14.- Continued.



(g) 645 planform.

Figure 14.- Concluded.

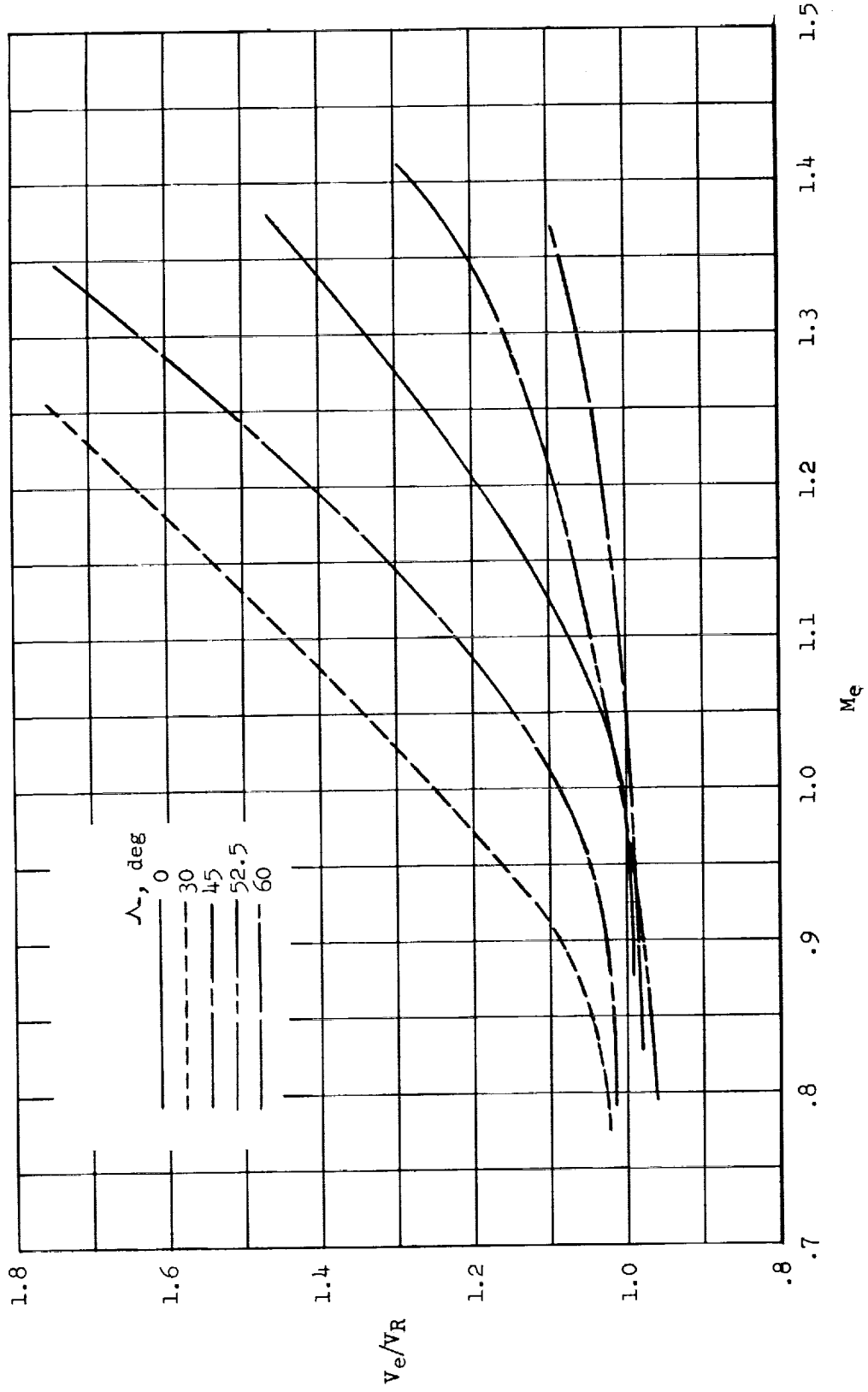


Figure 15.- Effect of sweepback on variation of flutter-speed ratio with Mach number for wings with aspect ratio of 4.

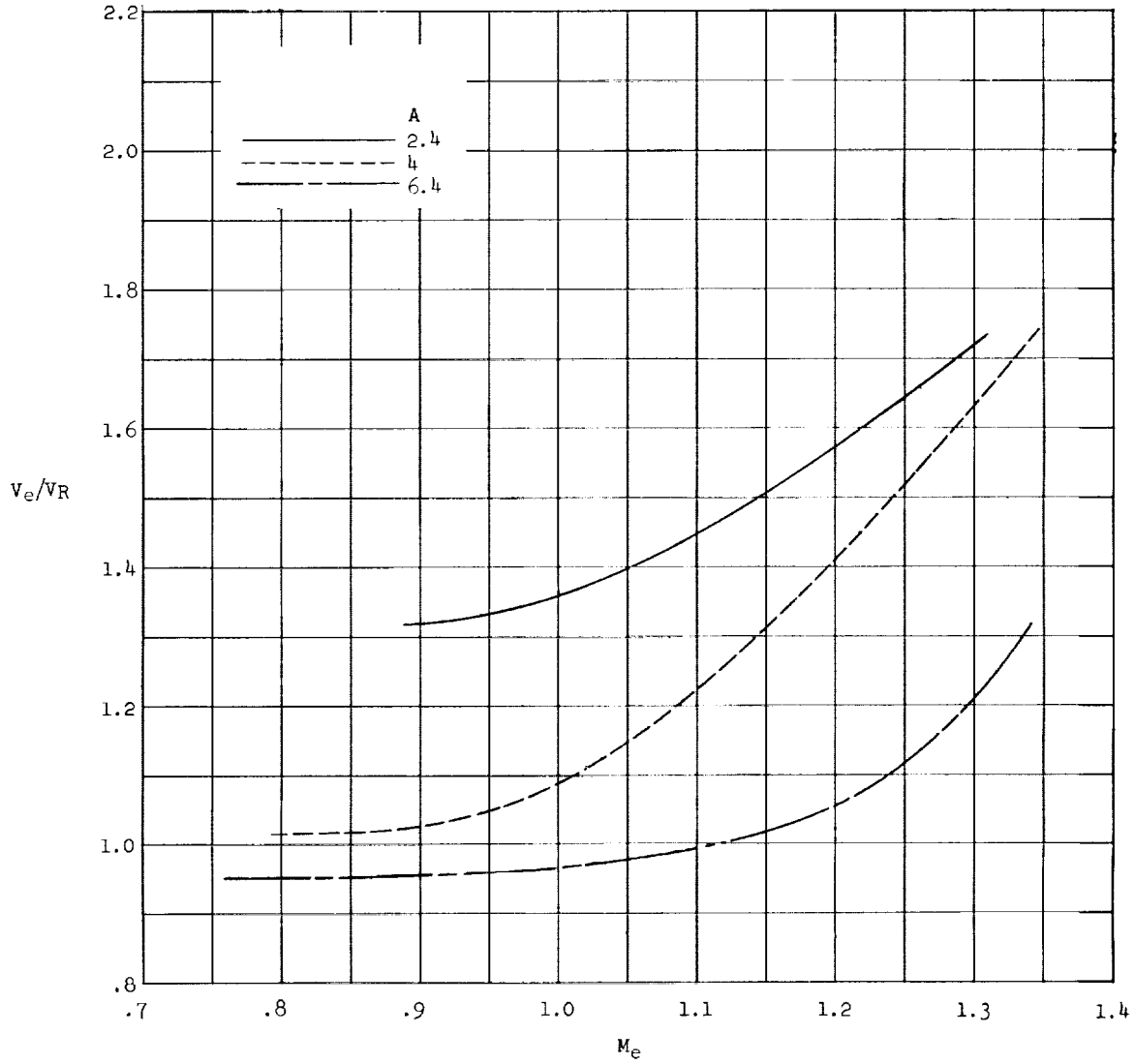


Figure 16.- Effect of aspect ratio on variation of flutter-speed ratio with Mach number for wings with  $45^\circ$  sweepback.

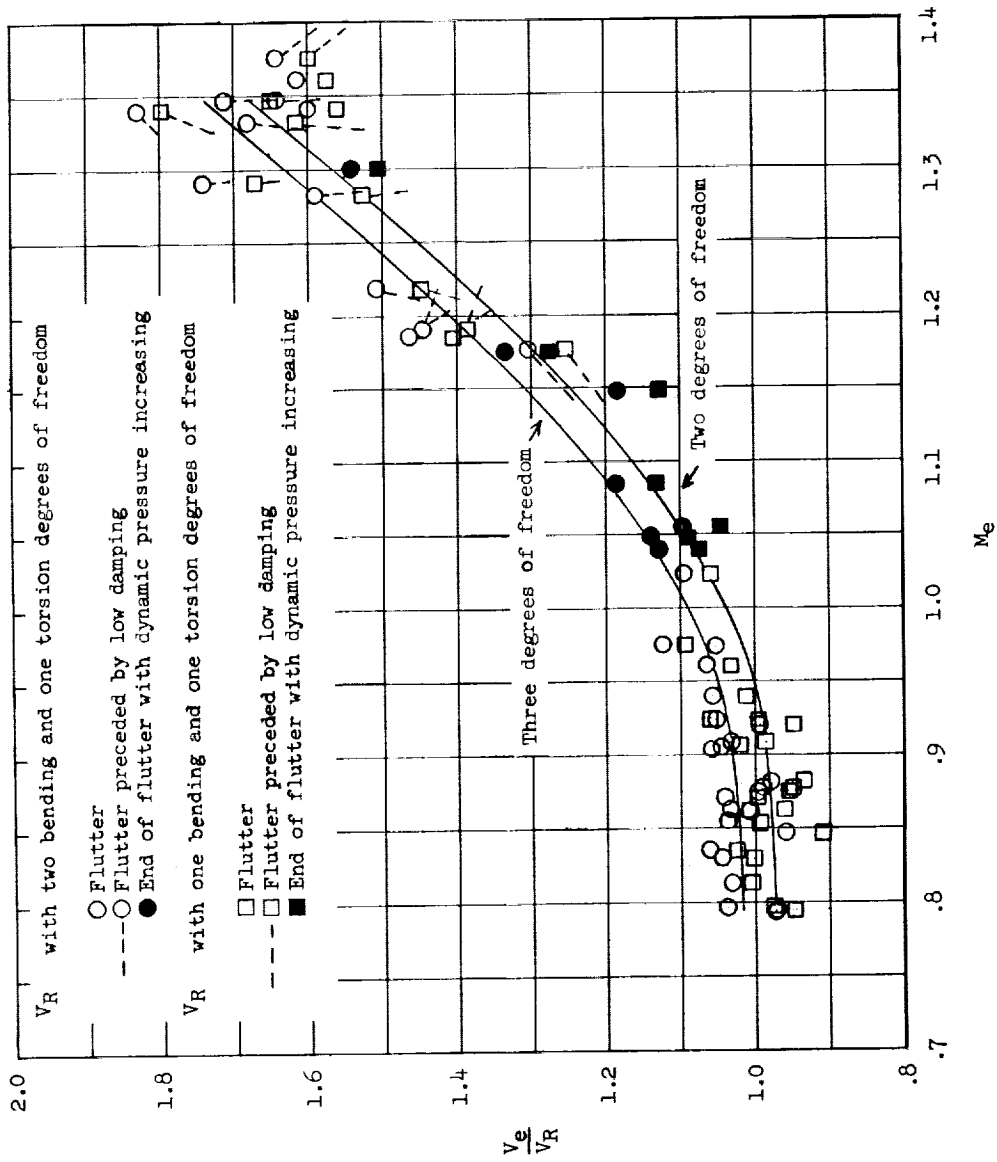


Figure 17.- Variation of flutter-speed ratio with Mach number for the 445 planform when two and three degrees of freedom were used in computing the reference flutter speeds.

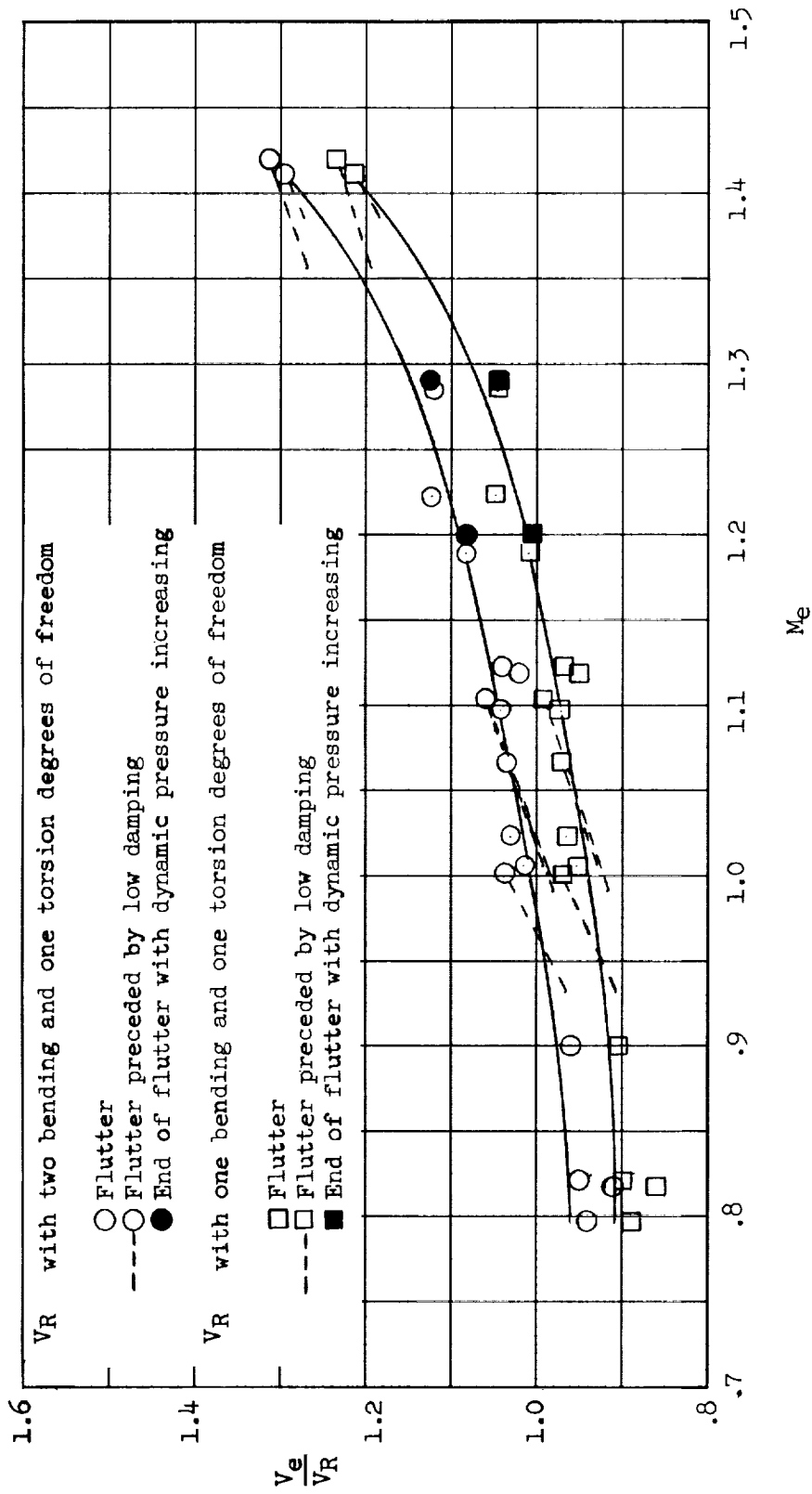


Figure 18.- Variation of flutter-speed ratio with Mach number for the 452 planform when two and three degrees of freedom were used in computing the reference flutter speeds.

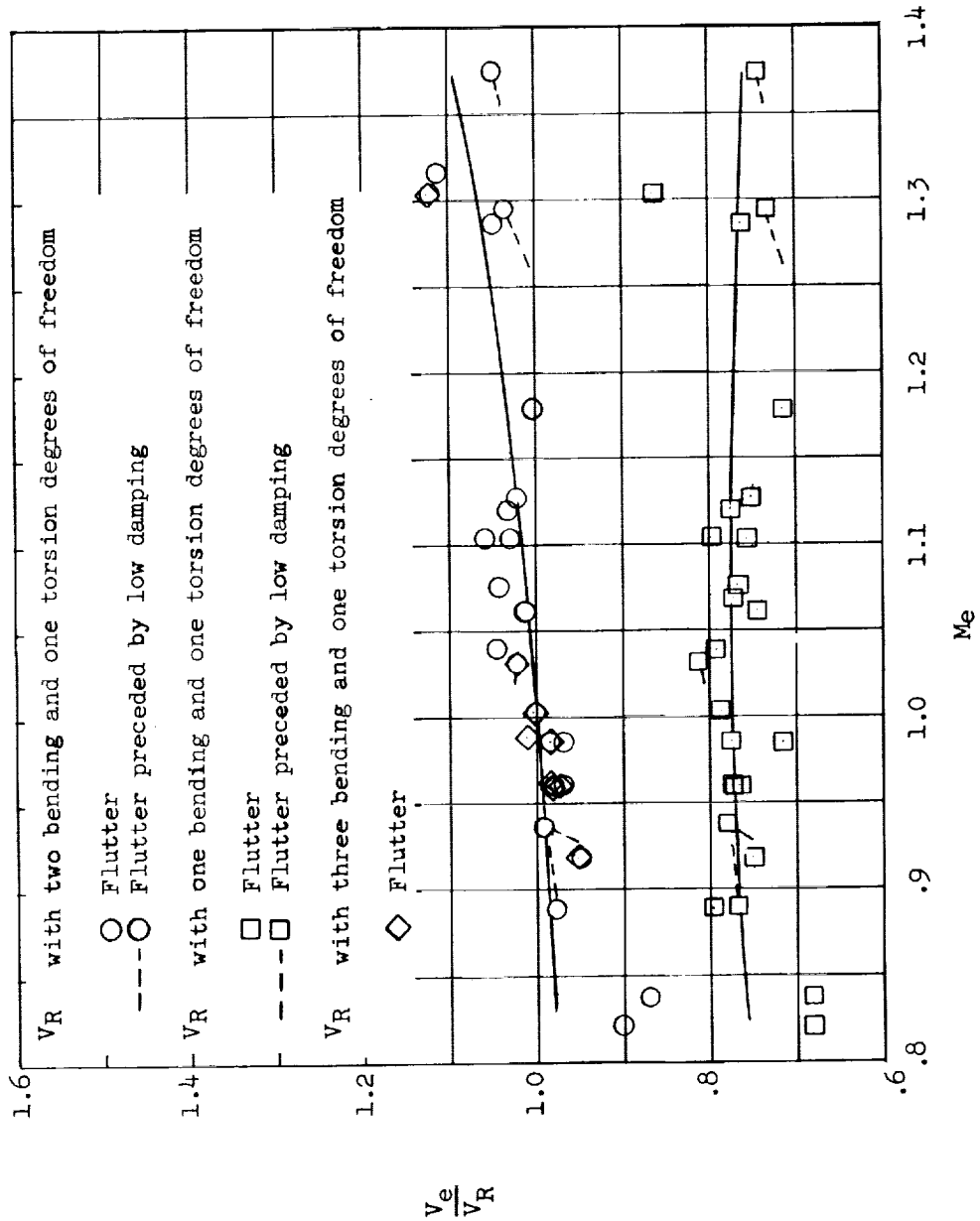


Figure 19.- Variation of flutter-speed ratio with Mach number for the 460 planform when two, three, and four degrees of freedom were used in computing the reference flutter speeds.

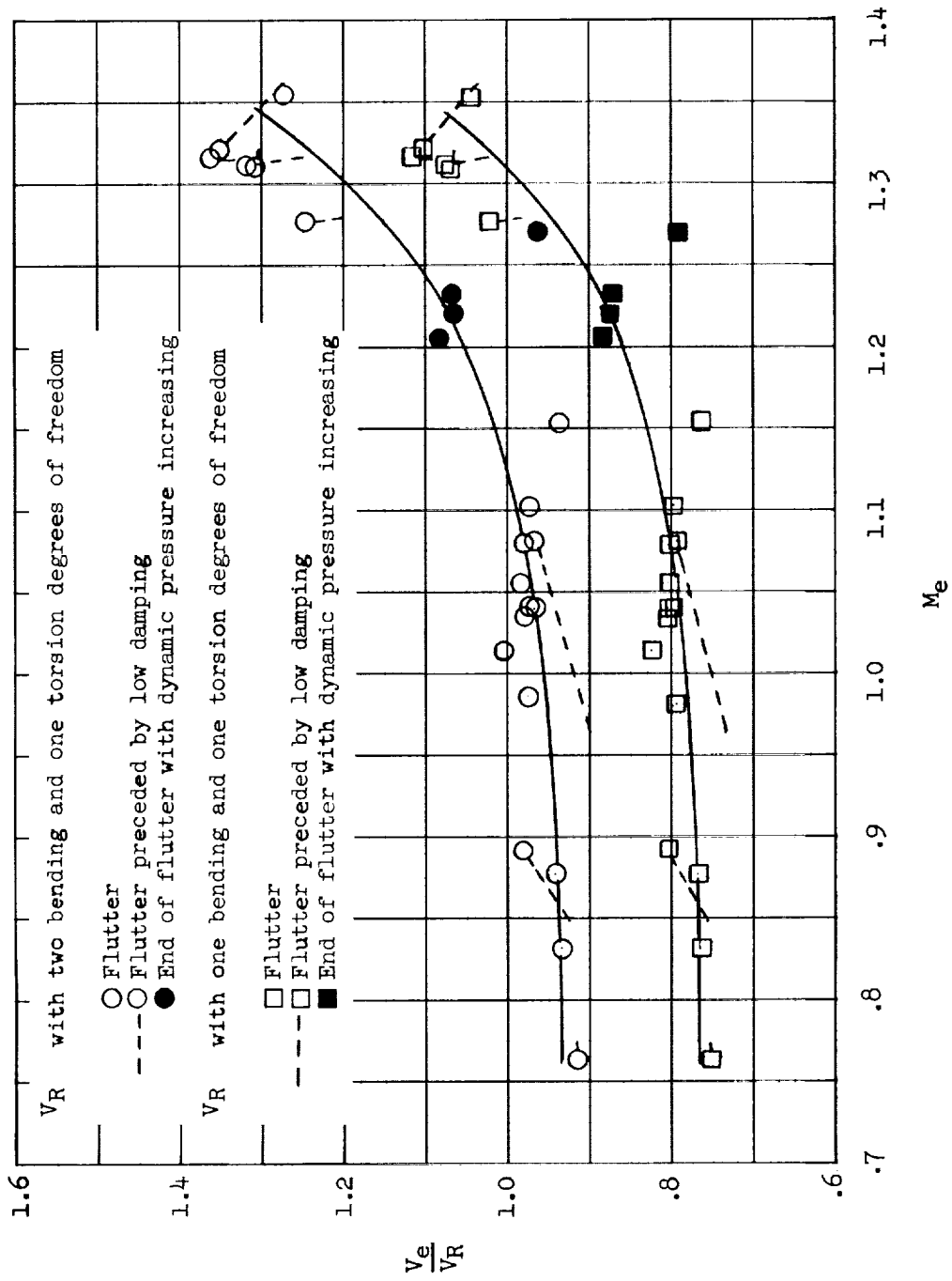


Figure 20.- Variation of flutter-speed ratio with Mach number for the 645 planform when two and three degrees of freedom were used in computing the reference flutter speeds.

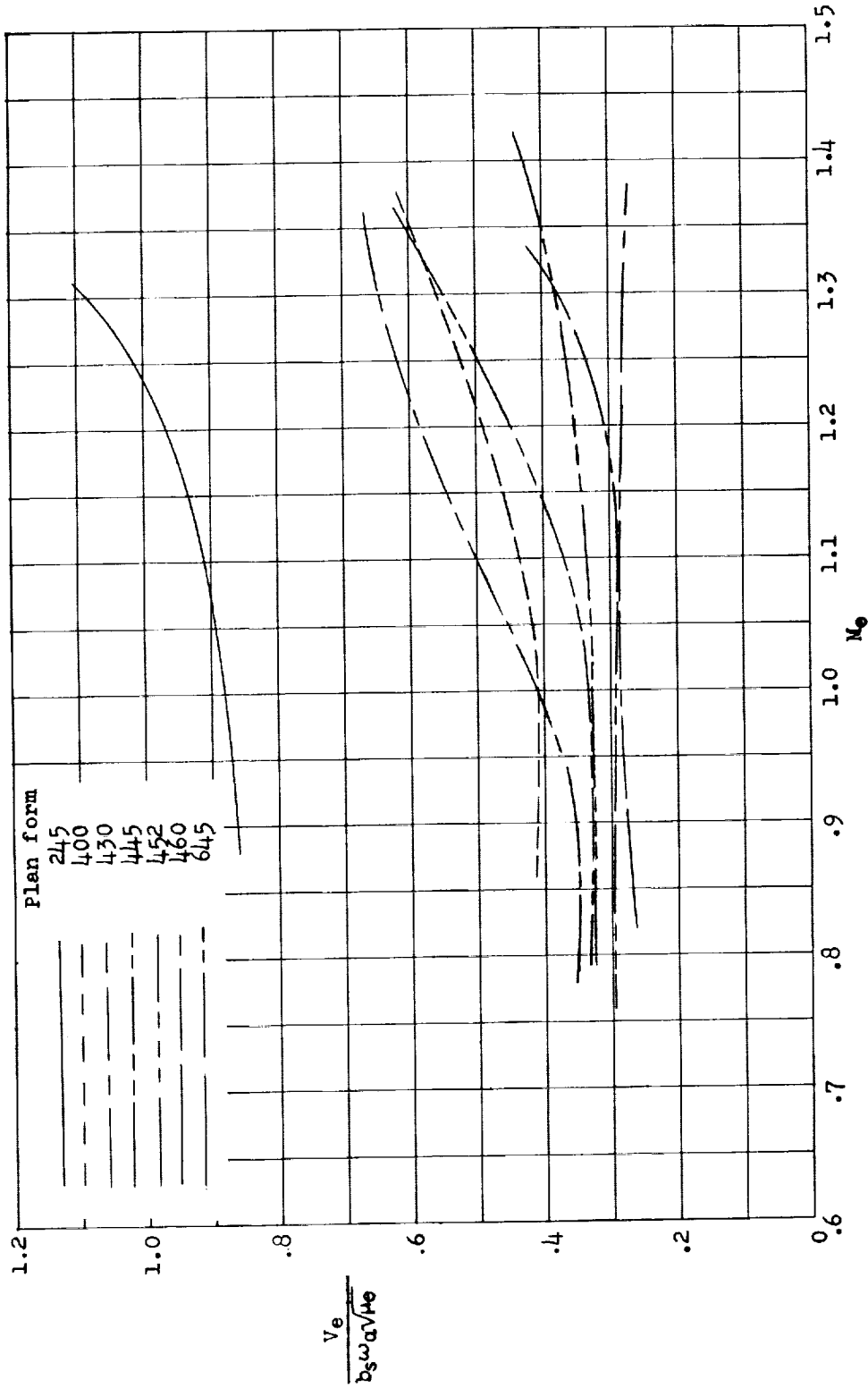


Figure 21.- Variation with Mach number of an experimental flutter-speed coefficient  $\frac{V_e}{b_s \omega_a \sqrt{\mu_e}}$  for plan-forms tested.

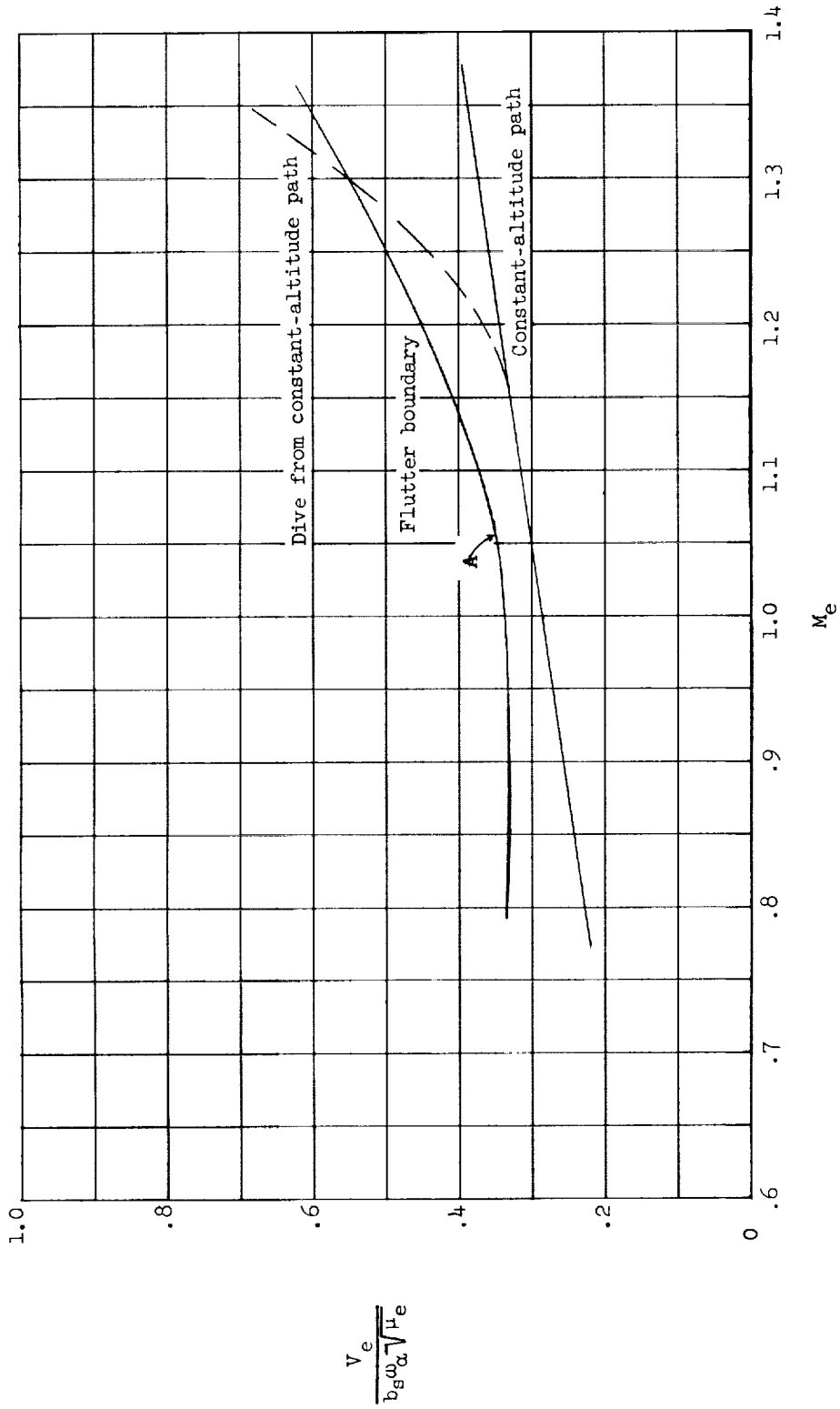


Figure 22.- Flutter boundary and hypothetical flight paths for 445 wing in terms of variation of  $\frac{V_e}{b_s \omega_\alpha \sqrt{\mu_e}}$  with Mach number.

